Energy Harvesting by Bio Inspired Fins Using Rectangular Cylinders of Different Aspect Ratio

By
Muhammad Haris

Regn Number
00000320976

Supervisor

Dr. Emad Uddin

SCHOOL OF MECHANICAL AND MANUFACTURING ENGINEERING (SMME)
NATIONAL UNIVERSITY OF SCIENCES AND TECHNOLOGY (NUST)
ISLAMABAD

(October, 2022)

Energy Harvesting by Bio Inspired Fins Using Rectangular Cylinders of Different Aspect Ratio

By
Muhammad Haris

Regn Number
00000320976

A thesis submitted in partial fulfilment of the requirements for the degree of

MS Mechanical Engineering

Thesis Supervisor
Dr. Emad Uddin

Thesis Supervisor's Signature: _____

SCHOOL OF MECHANICAL AND MANUFACTURING ENGINEERING (SMME)
NATIONAL UNIVERSITY OF SCIENCES AND TECHNOLOGY (NUST)
ISLAMABAD
(October, 2022)

Thesis Acceptance Certificate

Certified that final copy of MS thesis written by **Mr. Muhammad Haris**, Registration No. **2019-MS-ME-00000320976** of **School of Mechanical and Manufacturing Engineering (SMME)** has been vetted by undersigned, found complete in all aspects as per NUST Statutes/Regulations, is free of Plagiarism, errors and mistakes and is accepted as partial fulfilment for the award of MS/MPhil degree. It is further certified that necessary amendments as pointed out by GEC members of the scholar have also been incorporated in the said thesis.

Signature with stamp: _____

Name of Supervisor: Dr. Emad Uddin

Date: _____

Signature of HOD with stamp: _____

Date: _____

Countersigned by

Signature (Principal/Dean): _____

Date: _____

FORM TH-4

MASTER THESIS WORK

We hereby recommend that the dissertation prepared under our supervision by: Student Name Muhammad Haris & Regn No.320976 Titled: Energy harvesting by bio inspired fins using rectangular cylinders of different aspect ratio be accepted in partial fulfillment of the requirements for the award of MS Mechanical Engineering degree.

Examination Committee Members

1. Name: Dr. Zaib Ali Signature: _____

2. Name: Dr. Niaz Bahadur Khan Signature: _____

3. Name: Dr. Adnan Munir Signature: _____

Supervisor's name: Dr. Emad Uddin Signature: _____

Date: _____

_____ _____

Head of Department Date

COUNTERSINGED

Date: _____ _____

Dean/Principal

Plagiarism Certificate (Turnitin Report)

This thesis has been checked for Plagiarism. Turnitin report endorsed by Supervisor is attached.

Signature of Student
Muhammad Haris
Registration Number
00000320976

Signature of Supervisor

Declaration

I certify that this research work titled "*Energy Harvesting by Bio Inspired Fins Using Rectangular Cylinders of Different Aspect Ratio"* is my own work. The work has not been presented elsewhere for assessment. The material that has been used from other sources it has been properly acknowledged/referred.

Signature of Student

Muhammad Haris

2019-NUST-MS-ME-320976

Language Correctness Certificate

This thesis has been read by an English expert and is free of typing, syntax, semantic, grammatical and spelling mistakes. The thesis is also according to the format given by the university.

Signature of Student

Muhammad Haris

Registration Number

MS-ME-00000320976

Signature of Supervisor

Copyright Statement

- Copyright in text of this thesis rests with the student author. Copies (by any process) either in full or of extracts, may be made only in accordance with instructions given by the author and lodged in the Library of NUST School of Mechanical & Manufacturing Engineering (SMME). Details may be obtained by the Librarian. This page must form part of any such copies made. Further copies (by any process) may not be made without the permission (in writing) of the author.
- The ownership of any intellectual property rights which may be described in this thesis is vested in NUST School of Mechanical & Manufacturing Engineering, subject to any prior agreement to the contrary, and may not be made available for use by third parties without the written permission of the SMME, which will prescribe the terms and conditions of any such agreement.
- Further information on the conditions under which disclosures and exploitation may take place is available from the Library of NUST School of Mechanical & Manufacturing Engineering, Islamabad.

Acknowledgements

I am thankful to my Creator Allah Subhana-Watala to have guided me throughout this work at every step and for every new thought which He set-up in my mind to improve it. Indeed, I could have done nothing without His priceless help and guidance. Whosoever helped me throughout the course of my thesis, whether my parents or any other individual was His will, so indeed none be worthy of praise but Him.

I am profusely thankful to my beloved parents who raised me when I was not capable of walking and continued to support me throughout every department of my life.

I would also like to express special thanks to my supervisor Dr. EMAD UDDIN for his help throughout my thesis and for the AFM course which he has taught me. I can safely say that I haven't learned any other engineering subject in such depth than the ones which he has taught.

I would also like to pay special thanks to friends for their tremendous support and cooperation. Each time I got stuck in something, they came up with the solution. Without their help, I wouldn’t have been able to complete my thesis. I appreciate their patience and guidance throughout the whole thesis.

Finally, I would like to express my gratitude to all the individuals who have rendered valuable assistance to my study.

Dedicated to my exceptional parents and adored siblings whose tremendous support and cooperation led me to this wonderful accomplishment.

Abstract

In order to operate a micro electromechanical device, we need a small amount of energy. In this research, we suggested an energy harvesting system based on wake flow for these types of devices. Energy harvesting using piezoelectric flag is a renewable energy source which attain a lot of interest in the research field. The flag oscillates when the fluid force at certain velocity strikes the bluff body. It is positioned at the wake of the cylinder, and it functions as cantilever beam. When the water strikes the bluff body vortices is generated which tend to oscillate the flag and energy is transferred. The kinetic energy of the fluid is converted into electric energy using the piezoelectric flag and supplied directly to the small sensors when needed. Cross section area of the cylinders and different parameters strongly influenced on the power output. To investigate the impact of parameter on the energy harvesting, a flexible flag is used.

Detail experimentation was performed to investigate the influence of parameter with change in aspect ratio of cylinder on the power output. In this study, rectangular cylinder of different aspect ratio (1, 1.2 and 1.4) with bio inspired fins (Dorsal, Pectoral and Pelvic) were used. Apart from bluff body, other parameter like streamwise gap (Gx), stiffness of the flag and velocity plays an Important role in the energy harvesting. Total 63 cases were performed in our study and in each case 1 – 1.5min video was recorded to investigate the flapping of the eel. Total nine different type of cylinders was used in our study on which experimentation was done at different streamwise gaps. Streamwise gap (Gx) varies from 1 - 4. By varying the Gx we have found out that at some position the coupling of the wake with the piezoelectric flag is good enough and produce maximum strain.

The results concluded that by using Dorsal fins having 1.2 A.R rectangular cylinder gives maximum power. Maximum power was achieved at Gx = 3.5 which is 82.74μW. Minimum power was shown in 1 A.R rectangular cylinder in Dorsal fin at Gx = 1 which is 7.63μW. We had compared the hollow circular cylinder with our study, 5-10% more power was harvested.

TABLE OF CONTENTS

List of Figures

List of Tables

Chapter 1

INTRODUCTION

Energy harvesting is a newly developed technology which provide electrical energy sources to electronic devices and sensors which need less energy and some of them are wireless. This system of energy harvesting allows wireless health monitoring applications and supplying clean energy which helps in rise public safety. Contrastingly, this system is also beneficial in ecology, as it is minimizing the toxic and chemicals wastes by substituting the batteries. By the all the emerging researches on low powered wireless electronic applications, the energy harvesting system have enhanced [1-3]. The performance and design life of wireless sensor networks are notably effected by its batteries' weight and volume [4]. The studies [5-9] suggested that ambient flow/vibrational energy is supposed to be considered as appropriate for energy harvesting system and a main source of energy

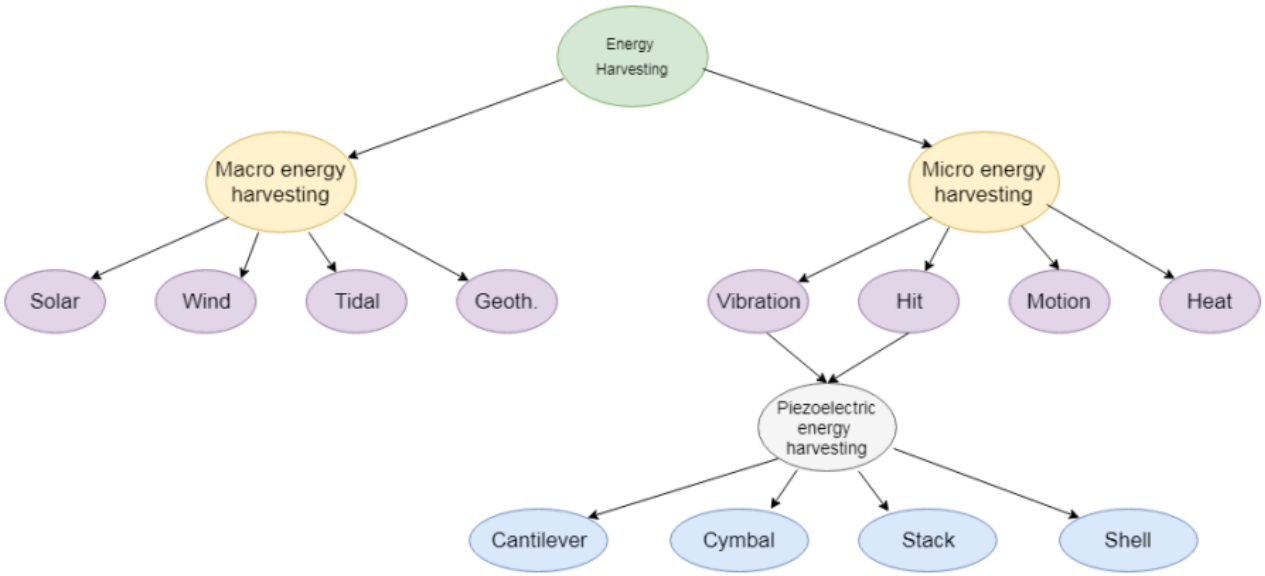

Figure 1.1 Renewable energy harvesting classification

1.1 Description of ambient flow energy

Till date, numerous methods are implemented for energy harvesting from ambient flow from the earlier of 1 Anno Domini (AD) [10]. One of the earliest methods of energy harvesting are Windmills, which are broadly used in 17^{th} and 18^{th} centuries in Europe as shown in Figure 1.2

Figure 1.2 Ancient wind turbine

They are widely known as clean energy power generators which convert wind power into electricity for around many years. As these equipment's are costly and only recommended where enough wind power is present, so it should preferably be not situated near any residential area. Furthermore, these windmills require substantial amount for maintenance and are only allowed to function when their effectiveness is above a threshold.

As a result of rapid decline in the of fossil fuels, ecofriendly energy sources drew all the attention and on the basis of prior windmill's mechanisms, now newly refurbished and technologized version of windmills are functioning in different parts of the world as shown in Figure 1.3

Figure 1.3 New wind turbines

The flowing air is the thrust force for windmills and the basic element of wind turbine is rotary propeller through which the energy is generated. Similarly, tidal turbines are also in consideration and works exactly same as wind turbines, but the only difference is the tidal waves, which is the force for their rotary propeller, instead of wind flow.

The ultimate method of energy extraction from flowing fluid is based on solid body's motion induced by contiguous fluid flow and this solid body and fluid's interaction generates the occurrence of fluid structure interaction (FSI). Considering the phenomenon of fluid structure interaction, various studies have been conducted by flow induced vibration for harvesting micro scale energy to power the independent power supply sensors for example an airfoil's coupled mode flutter [11-13].

Cylindrical bodies are commonly observed to swing back and forth while introduced to a fluid flow. In our daily routine life, few common examples of phenomenon of flow induced vibration can be seen like flapping of flag and pole of flag, tree crown, even a deep string holding a ferry standing inside water or power lines cables. The concept of flow induced vibration can be portrayed in these examples. This phenomenon is gaining all the attention and interest of scientific community every passing day because of possible availability of energy harvesting in it. The flow velocity, induce instability and time are the factors which tend to increase the amplitude, this behavior of the system is called aeroelasticity. The scale of instabilities possibly taking place results to be reasonably large even for the structures belongs to the civil and mechanical field.

Actually, if we consider the general sections of giant buildings and bridge, we can infer to variable side ratio rectangular cylinders which can be efficient and prone to more than one aeroelastic phenomenon under particular conditions. The bluff bodies are characterized by a non-streamlined cross-section, such as an airfoil. The boundary layer does not remain entirely intact to the whole surface, but it relies on a separation processes, in a bluff section. According to the local condition of the boundary layer the separation point is free to move on the surface in smoothly curved bodies and there is a change in its position according to the flow condition.

The oscillations start taking place in a structure by the contact with the fluid when a flexible structure is exposed to fluid flow, clearly witness in hydrodynamic and aerodynamic field. The flapping amplitude and oscillation frequency because of the force of fluid applied on the structure wholly depends upon the Strouhal number and Reynolds number.

1.2 Piezoelectricity

The piezoelectricity is a material that produces electric charge due to the applied outside pressure on it which results in deformation. Curie bothers discovered the piezoelectric material for the first time [14]. The limitation of their study was the generation of electric current from the deformed piezoelectric material, called as piezoelectric effect. A French scientist found that when the piezoelectric material is exposed to external electric charge, deformation occurs [15], and the outcome is known as “inverse piezoelectric effect”. The existence of natural Quartz crystals was learned in their research. Their conclusion was that the occurrence of natural dipoles inside the piezoelectric material is the actual reason behind the electric current generation from the existing natural piezoelectric material. The piezo material applications were based on this phenomenon. According to a specific group of piezo material, apart from that, the positive and negative charges formation varies [16]. When the generation of electricity from the electric dipoles are determined, we can know the production of direct and inverse piezoelectric effect. We can also determine the effect of different parameters on the piezoelectric energy generating proficiency of the material. When the positive and negative electrode in the piezoelectric material is coinciding with each other, means that the material is electrically neutral lacking the stress and deformation. The center of these both electrodes stretched or compressed, producing a current field within the material and generate the difference in voltage, whenever a stress or pressure is applied on the filament as shown in Figure 1.4. In order to conduct the charge from material to external circuit, the conductive wire is linked to positive and negative electrodes. In contrast with this notion, the neutral behavior of piezoelectric material is affected by the external electric field application and the internal electric dynamics of piezoelectric changes due to these electric field. The positive and negative electrodes travel in such a degree and coming back to their original neutral position, in order to refurbish the original position and neutrality of piezoelectric material. Thereupon inverse piezo effect is produced as the stress is induced and material is mechanically deformed.

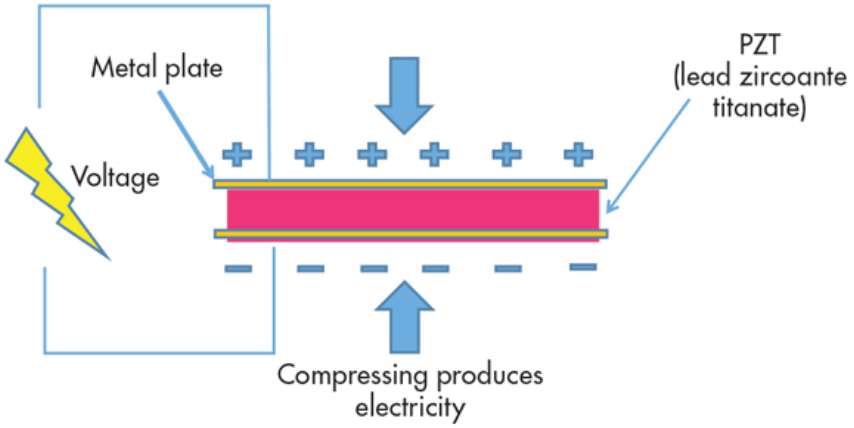

Figure 1.4 Working of Piezoelectricity Phenomena

The neutral form of crystal which means that the positive and negative electrodes of crystal are at a center and at a same point. The centers of the crystal distant in a vertical direction from each other that can be transmitted to external circuit and produce the electric field. Contrastingly, both the electrodes move in an opposite direction from each other causing deformation inside the structure, when an external electric potential is applied on PZT crystal

Moreover, the further categories of piezoelectric material are as follow:

1.2.1 Quartz

Quartz are present in the form of crystal and their crystalline properties and structure are limited to their transformation of shapes. This crystal has strong piezoelectric properties together with low sensitivity to temperature, atmospheric conditions and high stiffness. Their usage is valid in places where high deformation is essential and where more accuracy is necessary like in frequency control modules, electronic watches and microprocessor-based equipment.

1.2.2 Ceramics

Ceramics withhold some exceptional properties of piezoelectric with limited applications and high delicacy. The major advantage of this material is their accessibility in powder form and later can be converted into different shapes like cylinders, thin films or plates etc. Quartz contains more resilient piezoelectric characteristics than ceramics but transforming into any shape is the key factor for opting this kind of piezoelectric material.

1.2.3 Polymers

A piezo polymer which is commonly used is Polyvinylidene Fluoride (PVDF). They are naturally flexible and are soft compered to quartz and ceramics. They are weak in piezoelectric properties but because of their flexible nature they are mechanically stable and are used in numbers of application. They are typically found in thin filaments form and can be molded into required lengths. They are used in numerous experimental research works regarding generation of energy from piezoelectric materials due to their sustainability of large deformation.

1.2.4 Composite materials

When the flexible polymers and stiff ceramics are mixed, a different type of piezoelectric materials are formed which have both rigid, soft and flexible at the same time. Composite material can be used in research studies where large deformation is necessary because of those structural properties.

1.3 Why did author select PVDF flag for energy harvesting?

The motivation for the selection of piezoelectric flag for energy harvesting is due to the presentation of large amplitude motion with high flapping frequency related to the dynamics of flapping flag's features.

Flapping of piezo flag of such kind implies the perpetual energy exchange within the piezoelectric flag and adjacent fluids. This energy exchange mechanism is getting a lot of attention by different researchers, and they are chasing down different methods from which the energy is cropped from this mechanism. Commonly there two different techniques from which energy is extracted using flag-based energy harvester.

- Energy is produced from the displacement either [17]
- OR by the deformation of the flag [18, 19]

The studies based on active piezoelectric material are opting the second method [20-22].

1.4 Motivations

As our fossil fuels are continuously decreasing and environmental changes are affecting our fossil fuels badly, human need energy for the survival that's why scientists are in search of developing new methods and technique extricate energy from different natural resources which are present in abundant. Different renewable energy resources like solar

energy, wind energy, hydro turbines etc. can be used to produce electricity. Hydro turbines work on the principle of extricating energy from the motion of water waves which is then transferred to generators. Now new techniques have been found by the scientists to produce cost efficient energy by using some advanced materials

Compact sensors can extract power from there environment to accomplish different health and military tasks. Monitoring of different health structures will allow the person to repair all the damages before time and it saves cost and time. To execute different on field tasks, MEMS (micro electromechanical systems) are being created which is a very power efficient and being used in different communications systems. Wireless communications, advanced sensors and different data transmission systems are being installed in micro electromechanical systems which needs a source of power to operate. Power lines or batteries can be a constant source of power supply.

Nevertheless, MEMS systems also have some disadvantages like environment get effected by disposing off those battery and they need replacement after some time. Actual task is to provide power to MEMS systems because they were mostly used at that place where people cannot be easily reached, so battery replacement is an issue. An idea to solve that task is to provide a source of energy nearer to those devices. Energy harvesting system from thin eel placed in a wake of a bluff body which is moved by vortices. The effectiveness of that energy harvesting depends upon the bluff body which can be of different shape, the flow of the water and physical parameters. So, we studied the effect of different bluff body on thin piezoelectric membrane (eel) and geometric parameters too.

Our aim is to increase the power and strain energy by the movement of eel using the water tunnel in the laboratory. Applications such as bridges and other structures in water have a lot of energy which we can use to power up small devices. These sources provide energy all day which can resolve the issue of constant power supply to micro electromechanical devices

1.5 Research Aim

The aim of this study is to investigate the effect of shape change by adding fins on the rectangular cylinders and to increase the energy output by using these cylinders.

1.6 Research Gap and Objectives:

No research has been carried out in the past to enhance the energy output by bio inspired fins using rectangular cylinders of different aspect ratio.

- To analyze the effect of using different aspect ratio cylinders having bio-inspired fins on energy harvesting.
- To discover the best-suited fin configuration on the rectangular cylinder for energy harvesting.
- To study the effect of different parameters like streamwise gap in x-direction on energy harvesting.
- To make comparisons between different rectangular cylinder configurations having fins for higher power output.

Chapter 2

LITERATURE REVIEW

Conventional energy resources are quite used by a huge number of populations, leading to the discharge of greenhouse gases, global deforestation, global warming and eventually they have negative effects on human health and environment [23]. Contemporarily, reusable resources of energy are gaining attention. The desire of discovering these energy resources that can act as an alternative source of fossil fuels and produce ecofriendly energy has been the main topic of researchers in the recent decades [23]. Harvesting an unused energy from the ambient fluid flow is present in plenty amount in a natural environment due to this there is a drastic change in environment and the energy consumption in daily life. Researchers are interested in altering it into a useful electric energy for the past decade. The primary focus of the research has been diverted to the development of renewable and maintainable energy sources from the conventional fossil fuels, in the recent times [23]. Because of this a swift up-gradation in electric system is perceived as the microelectromechanical systems (MEMS) develops, wireless sensors for observing structure health [24], sensors for industrial systems and there is an increase in the demand for energy-efficient equipment. Those technologies which are self-powering can store energy without batteries and can effortlessly be held in remote locations without the monotonous process of replacement of batteries in low power electronic devices as it can be tiresome and expensive and no need for the maintenance also. These can be used trickle charging of current batteries as modern sensors function at very low power so supplementary items can be ignored which consequences in operational cost reduction [1, 2, 25, 26]. The use of micro sensor power is reduced by the new development in the field of MEMS and electronic sensor device. To function properly, these sensors need a few microwatts of energy. Consequently, these sensors or the harvested need a few microwatts of energy to operate appropriately. Thus, the piezoelectric material is used to harvested energy or these sensors at small scale is enough to operate them efficiently like quartz watch, wireless sensor node for structural and human health monitoring [8, 27, 28]. By the use of multiple piezoelectric membranes in enhanced circuit design, the harvested energy can be increased (65, 66). So, to assimilate the autonomous power source with such devices rather than conventional battery packs is much easier. This method is environment friendly and also lessen operational and maintenance

costs [1, 2, 25, 26, 28, 29].

A device to transform mechanical energy into electrical energy is provided by the harvesting energy from piezoelectric devices that can substitute conventional battery packs. Few research in the near past were conducted to organize piezoelectric material as a source of green energy like temperature sensors, road pavements, humidity and charging watch [28], [29-32].

Numerous types of unutilized energy exist in the environment, such as thermal and fluid flow, solar, acoustic and mechanical can be extricated using different transduction mechanisms like electrostatic [33],electromagnetic [34] and piezoelectric [35]. Amid these, the popular ones are vibration/pressure driven energy harvester and due to their feasibility of application like efficiency, high energy density and miniaturization perspective are extensively studied [36]. There are sufficient advantages of piezoelectric transduction over its counterparts and acquired attraction of researchers for harvesting energy from cantilever beams and emerging small scale energy harvesters to power up the devices which are self-bearable and sensors in unapproachable areas [35].

A common nature occurrence of an interaction between the vortex and the flexible flag in wake of a bluff body and also in engineering fields. The environmental influence and limited availability of fossil fuels persuade the development of reusable energy resources. Significant efforts are determined on the use of renewable energy from natural resources such as geothermal heat and biomass, water, tides, rain, wind, and sunlight. Renewable energy from wind, geothermal, hydro, biofuel and biomass is considered to be globally energy consumption of 5.8% in 2012, which was then increased to 11% in 2018 [37].

In the current passing years, the flapping motion of a piezoelectric membrane positioned in the fluid flow of energy harvesting has gained a lot of attention. Several studies were proposed for this purpose. Hence, to have an appropriate understanding into the dynamics, key parameters and corresponding output of the piezoelectric membranes are useful [38]. To extract an energy using vortex-induced vibration, is a possible source of renewable energy. The usage of energy flow by altering it to electric energy with the help of piezoelectric membrane was proposed by Smith and Allen [18]. The vibrations, vortex-induced vibration (VIV) or flow-induced vibration (FIV), of flexible piezoelectric membranes were observed which have large flapping amplitude and oscillation frequency is beneficial in diverse arrangements like placing a flexible flag in conventional or in inverted orientation [32, 39, 40].

Driving forces are required by piezoelectric energy harvesters that could possibly stimulate the membrane with kinetic energy present in the fluid flow which are divided into four categories, buffeting, vortex-induced vibrations (VIVs), flutter and galloping [41].

The mechanical power and strain energy by stimulating the membrane through vortex-induced vibration in the wake of a rectangular bluff body optimized by Allen and Smits. The joining of the unsteady flow field with the oscillation flapping of the membrane can produce resonance in flowing fluid resulted in high energy harvesting [42, 43].

By shifting the mass ratio, aspect ratio, stiffness and Reynolds number numerous arrangements were developed for energy harvesting from vortex-induced vibrations in the water/oceanic environment (9-14). A comprehensive assessment was made by Wang et.al. [41], as they illustrated various techniques and models of harvesting energy for flow-induced vibrations.

Efforts are being made, for the past few years, to establish the mechanism that can harvest the energy from a membrane in forced motion like in a wake of a bluff body a flexible piezoelectric member is placed. Researchers provided an experimental demonstration of the process a membrane is placed in the wake of bluff body, for a continuous energy harvesting from a flexible polyvinylidene fluoride (PVDF). In this process, a periodic flapping of the membrane was induced by a substitute variation of the Karman vortex street. The optimal coupling between the wake flow and energy harvest as the resonance condition was proposed by Allen and Smith [18] where Karman vortex street is minimally effected by the membrane's damping. Hu et al. [44] have given the analytical solution in numerical results with experimental validation for the finest position of piezo energy harvester. Approximately 17.8% increase was reported with a numerical model in electromechanical conversion efficacy held by experimental work by means of piezoelectric flag [45].

Akaydin et.al. [42] arranged a highly rigid piezoelectric beam in the wake of a cylindrical bluff body with start and end both the edges were kept fixed and free correspondingly and vibrations were observed at the first node with continuous-voltage output in even episodes. Dingyi et al. [45] proposed the purpose of flexible plate's displacement in front of a D shaped cylinder.

A dead fish movement can be shown like a flapping flag, in the wake following a bluff body, can push forward itself upstreaming by vortices which is similar to flow energy extraction by the use of a piezoelectric flag. During this a shove is formed in the upstream parallel direction to kinetic energy extraction from the flow. Researchers explained that when the forces are applied on the piezo-beam, they have a positive interaction with the flow speed

and the bluff body's diameter, 17% voltage generation achieves electromechanical efficiency and increased up to 71% and 110% by use of hybrid energy harvesting system [46] and a moveable bluff body [47] particularly for energy harvesting. The researchers worked on the depletion of mechanical losses and stated that mechanical efficiency is increased 90% by damping ratio, mass ratio, and Reynolds number , tuning [48]. A range of piezoelectric flag without a bluff body were used in different directions to incoming water and the auspicious results were showed in experiments and the possibility of energy harvesting which formed motion of water. Hobbs et.al [49] A research has been carried out for the use of a range of cylinders and drew the attention towards the optimal spacing and flow speed to harvest energy, similarly, by the use of vortex-induced vibration, the optimal position in cylinder wake for a flapping sheet is found [44]. The limitations of low toughness and thin flow velocity by means of force increase in magnetic coupling were explained by Zhao et.al [50].

Zhang et. al [51] anticipated that a power output of 803.4μW can be achieved by using of an interference cylinder of different cross-sections and attained for a square cross section at non-dimensionalized stream-wise gap 0.9 and 2.36m/s of velocity flow, and the increase of 380% can be seen in an organized region by the addition of interference cylinder. Researchers tended to use the tandem arrangement for the interface behavior, positive and harmful modes, enhance the efficiency of energy harvesting system and hydrodynamic drafting and. Shan et.al. [52] presented that 167.8μW power output was accomplished at the water flow with the velocity of 0.306m/s and the ratio space (L/D) of 2.5.

Many researchers did experiments on water tunnel and use wake galloping for energy harvesting for a variety of flow speeds and spacing among the cylinders for which piezoelectric aero elastic energy harvester based on galloping can be used efficiently for the system. The results revealed that rise in the array of working flow speed, cut-in-speed and simple galloping was replaced by improved energy output [27, 53].

The enhancement of time-dependent tension in the energy harvester depended on the unstable forces of flowing fluid which by adhering a bluff body directly at the free end of the piezo-beam. An uneven pressure supply arose due to vortex shedding on its surface that is a source of changing it and producing strain in the harvester [54-59]. Hu et.al [44] demonstrated an experimental research by altering circular cylinder and adding a small diameter rod into it to enlarge the unsteady region in different circumferential angles in order to enhance the ability of energy harvesting by connecting to the free end of the beam. The researchers altered circular cylinder with a Y-shaped connection and described the conversion of vortex-induced vibration into galloping for energy harvesting and done simulations for

results comparison Wang et.al.[60].. The flapping flag shows flutter and it goes into limit cycle oscillation after a critical speed that resulted in a huge amplitude motion applies energy harvesting at low frequency and with huge oscillations [61, 62].

Different cross-sections of bluff bodies like a rectangular, triangular prism, circular, square, pentagon, qusai-trapezoid and cir-tria prism were used to boost the energy harvesting, which showed the increase of 26.5% and 45.7% in efficiency statistically [64, 65]. Nevertheless, such numerical models did not offer an accurate estimate of harvested power, insufficient experimental validations and were limited to 2D simulations. The interference cylinder with various aspect ratio were proposed by Zhang et.al. [51] in order to boost the transverse vibration which results in greater voltage output. A constantly small amount of energy was harvested by altering flow energy into electrical energy. Several studies were performed in order to raise its effectiveness and examining the dynamics of flag with and without a bluff body. Zhang et.al. [51] explored by experimentation that the resonance impact on energy harvesting with unusual attributes of Strouhal number, variation in coefficients of lift and drag. Song et.al.[29] presented the comprehensive numerical analysis which was complying with their experimental findings and observed the highest power of 84.49 μW with 60.35mW/m^2 energy density at 0.35m/s velocity with resonance vibration. For a better performance, they suggested a large diameter of connected cylinder and small mass weight.

Various studies were conducted in order to enhance the performance of energy harvester by amplifying the cross section and shape of the bluff body. This change in shape was first experimentally examined in the wind tunnel by the use of a T-shaped bluff body and gained an uninterrupted electric power of 4mW at 4m/s [66]. Zhang et.al. [64] explored various shapes of bluff body statistically like square prism, circular, pentagon prism, cir-tria prism and triangular prism and determined that by the use of cir-tria prism shaped bluff body a 26.5% of energy harvesting increases, conversely, a unfortunate performance was given by the square shaped cylinder as compared to other cylinders. For an effective galloping, the idea of obtuse angles isosceles triangle presented the rules for constructing a triangle bluff body [67]. A bluff body of three-blade with Y-shape cross section was explored experimentally, square shaped bluff body's output voltage was compared and revealed that when a half-angle of blades were set in the middle of 600-800, a highest amount of voltage was achieved [59]. Energy harvesting performance of four cylinders shapes like q-trapezoid, circular, square, and triangular was statistically investigated by Ding et.al. [65], for an extensive range of Reynolds number 10,000-13,000 and concluded that a variation in shape can enhance results, also, for q-trapezoid, they gained a peak harvesting efficiency at Re =

60,000.

Bluff body shapes were altered for a huge quantity of energy harvesting by the use of combined galloping and VIV phenomenon [59, 60, 64, 68-70], but the wake produce impact on piezo-flag and its dynamics as the piezo-flag was secured with the substrate, was not found.

Zhang et.al.[71] suggested that for enhancing the output of energy harvesting, the interference cylinder is used, by fixing it and altering its streamwise gap from the primary cylinder along with the flow of velocity. Numerous studies, which were founded on experimentation and simulation, concluded the consequence of flag orientation and arrangement like staggered, tandem side by side and multiple flags, which exhibited a connection with the arriving flow accompanying positive and negative interface of vortices [32, 39, 72-74]. To enhance the functionality of these energy harvesters, different techniques and configurations were recommended which involves the variation of the bluff body by altering it into equilateral prism-shaped, Y-shape , Arc shape and T –shape [59, 60, 66, 68-70, 75]. Previous studies did not place easily the piezoelectric flag inside the wake region as it was attached on the beam/substrate which was linked to bluff body directly.

Though there are various studies with various phenomenon but the purpose they are debated here is to emphasize the point to switch in shape of a bluff body has a considerable impact and the efficiency of energy harvesting system is enhanced.

Therefore, no research has been carried out by using the bio inspired fins using rectangular cylinder of different bluff bodies. By placing the cylinder and the membrane in the horizontal direction and changing the streamwise gap (Gx) will affect the output power. So, by adjusting the flow of the water tunnel constant and changing the streamwise gap will increase the flapping amplitude and oscillating frequency which results in high power generation. For the best results we will compare our experimental results with the baseline case which is hollow circular cylinder.

Chapter 3

EXPERIMENTAL METHODOLOGY

3.1 Water Tunnel Setup

All the experiments were performed in water tunnel present in NUST Islamabad. National University of Science and Technology (NUST) has a wide range of labs present in Department of Mechanical Engineering SMME. The water tunnel was closed circuit and operated at low speed. Experiments has been carried out at a cross sectional area of (L x W x H) 2000 x 400 x 400 mm. A motor was attached with the tunnel to control the speed (U_∞) of the water under a range of 0 - 0.5m/s. Motor used was VFD-Variable Frequency Drive. To make the flow laminar a honeycomb with hexagonal openings used having a size of 1830 x 500 x 25.4 mm.

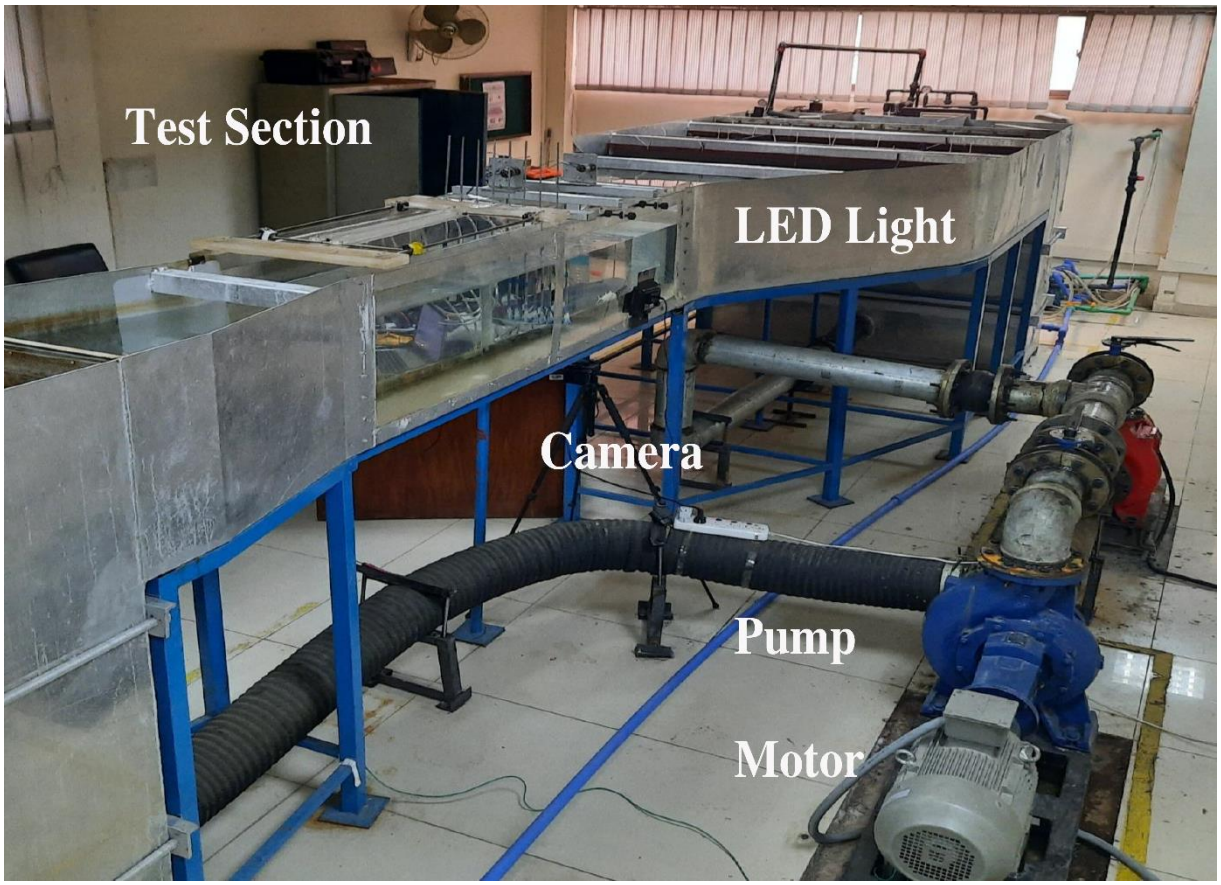

Figure 3.1. Closed circuit water tunnel

3.1.1. Boundary layer thickness:

When the local velocity has a achieved a point where the flow become asymptotic to the distance normal to the wall of the test area is known as boundary layer thickness. Across a flat plate, laminar boundary layer can be formed which is related to Blasius conditions, it is represented by δ_{99} and calculated by:

$$\delta_{99}(x) \approx 5.0\sqrt{\frac{\nu x}{u_o}} \qquad (0.5)$$

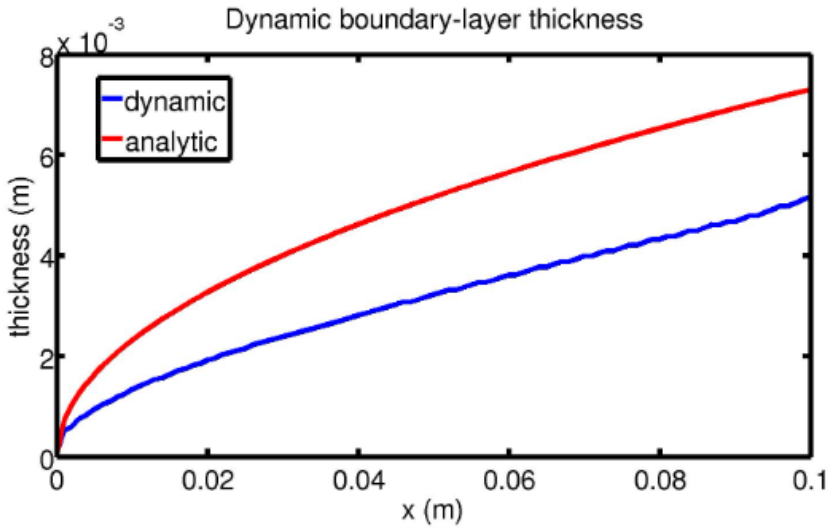

Figure 3.2. Boundary layer thickness and length "*x*"

It is very important to measure the boundary layer thickness because it gives the appropriate position where we place the bluff body inside a test section. As shown in figure 3.2, boundary layer increase with increase in length. This graph shows us the exact range where we need to place our energy harvesting system.

3.1.2. Turbulence Intensity:

In a fluid flow, the quality of the flow is dependent upon the turbulence level. Turbulence intensity is defined as a ratio of root mean square velocity to the mean velocity.

$$I = \frac{u_{rms}}{U}$$

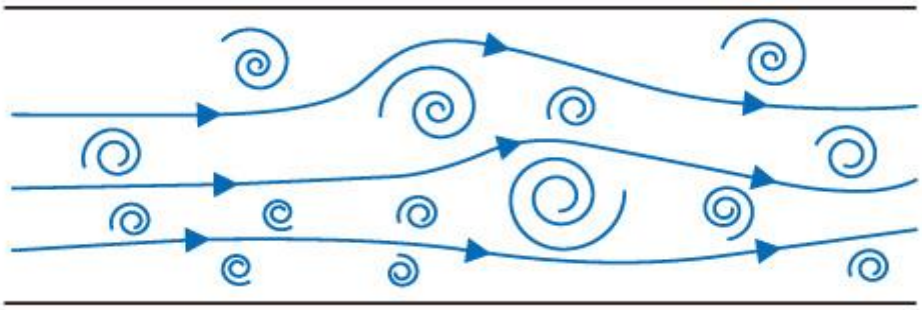

Figure 3.3. Turbulent flow velocity

In water tunnel, the turbulence intensity is less than 1%. It shows that our experimental results will not be affected, and quality of the flow is good enough. Turbulence intensity is further defined as:

- In closed shape machines like heat exchangers and turbines, high turbulence is noted because velocity of the flow is very high. In our case it will remain in between 5% - 20%.
- In large pipes like monopile and chimneys, medium turbulence intensity is noted which is approximately 1% - 5%.
- When the fluid pass from a point which is halt like in a car, aircraft etc. low turbulence is noted. In a water tunnel, we have experienced a low turbulence intensity in our study.

3.1.3. Material Selection for Rectangular cylinders:

Rectangular cylinders were 3d printed. In 3d printing PLA Plastic material was used. Polylactic acid also known as PLA which is very important material used in 3D printing. It is better than Nylon and ABS. It has greater strength and stiffness and a user-friendly thermoplastic. Mechanical Properties of PLA Plastic is shown in Figure 3.4

Properties	Units	ASTM	Common Material	
			PLA	ABS
Tensile Strength	MPa	D638-03	59	40
Elongation at Break	%	D638-05	7	50
Modulus of Elasticity	MPa	D638-04	3750	2600-3000
Izod Impact Strength	J/m	D256-06	26	34
Density	kg/mm^3		0.00105	0.00125
Cost per kilogram	Rand/kg	-	R 900	R 900
Colour		-	Various	Various

Figure 3.4. Mechanical Properties of PLA

3.1.4. Material Selection for Flag:

PVDF (Polyvinylidene Fluoride) flag is very flexible, and it can easily transform into any driving element shape (See Figure 3.5). It is nontoxic in nature and better than PZT material. Specification of this flag is DT2-052K/L, P/N: 2-1003744-0, w/rivets. It has come with the lead to acquire energy harvesting data. Its trailing edge is free and leading edge is attached with an aluminum rod. The aluminum rod has a diameter of 4mm. The active length and thickness of the flag is 62mm and 64µm. The overall dimension is 72 x 16 x 0.181mm (See Table 3.1). A transparent plastic sheet is wrapped to protect the flag. The upper part of the aluminum rod was fixed with the same structure on which all the cylinders are mounted.

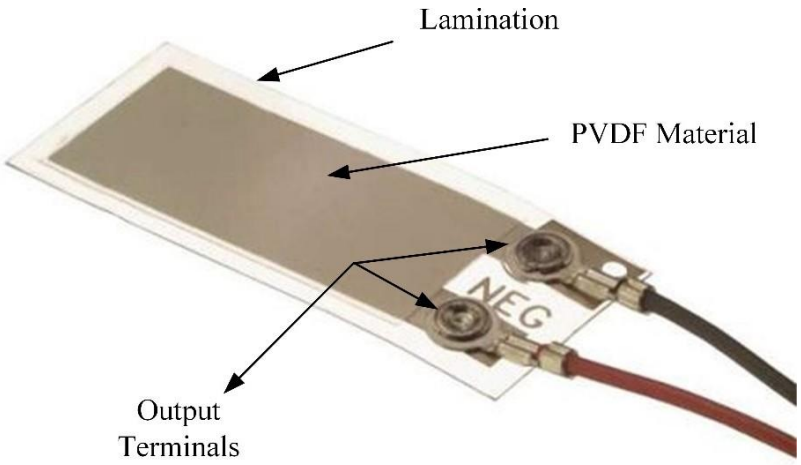

Figure 3.5. PVDF Flag

Material	PVDF
Size	72 mm x 12 mm x 64 µm
Membrane thickness	28 µm
Poisson ratio	0.46
Young's modulus	1.38 GPa
Capacitance	1.44 nF
Density	1.78 kg/m^3
Voltage range	10 mV – 100 V
Operating temperature	0 °C to +70 °C

Table 3.1. PVDF Properties

3.1.5 Measurement of Energy Harvesting:

All the rectangular cylinders were made up of PLA plastic material. There were three different types of rectangular cylinders having different aspect ratio used in our current study. Aspect ratio is defined as a ratio of length to width. The wall thickness of all the cylinders was 2.5mm. In our current study the length of all the cylinders was kept constant which was 25mm whereas the width was changing in each cylinder. That's why the aspect ratio was changed in each of the cylinder. Dimensions of all three cylinders are shown in Figure 3.6

(a) (b) (c)

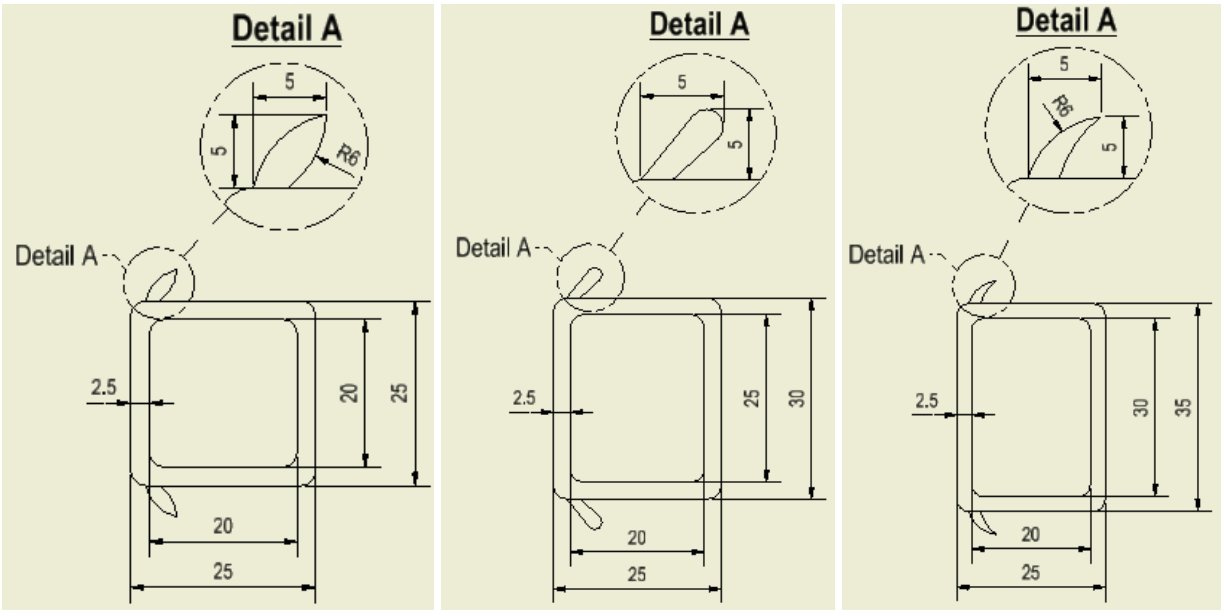

Figure 3.6. Rectangular Cylinder and Fin Dimensions. (a) 1 A.R cylinder with dorsal fins (b) 1.2 A.R cylinder with pectoral fins (c) 1.4 A.R cylinder with pelvic fins

Now there was three different type of fins which were attached with these cylinders i.e., Dorsal, Pectoral and Pelvic. The concept of the fins was taken from the field of biomimetics. The fins of the fish were similar to the fins we used in our study. The height of all the rectangular cylinders was 400mm. So, three different type of cylinders and three different shapes of fins make nine various combination of cylinders (See Figure 3.7).

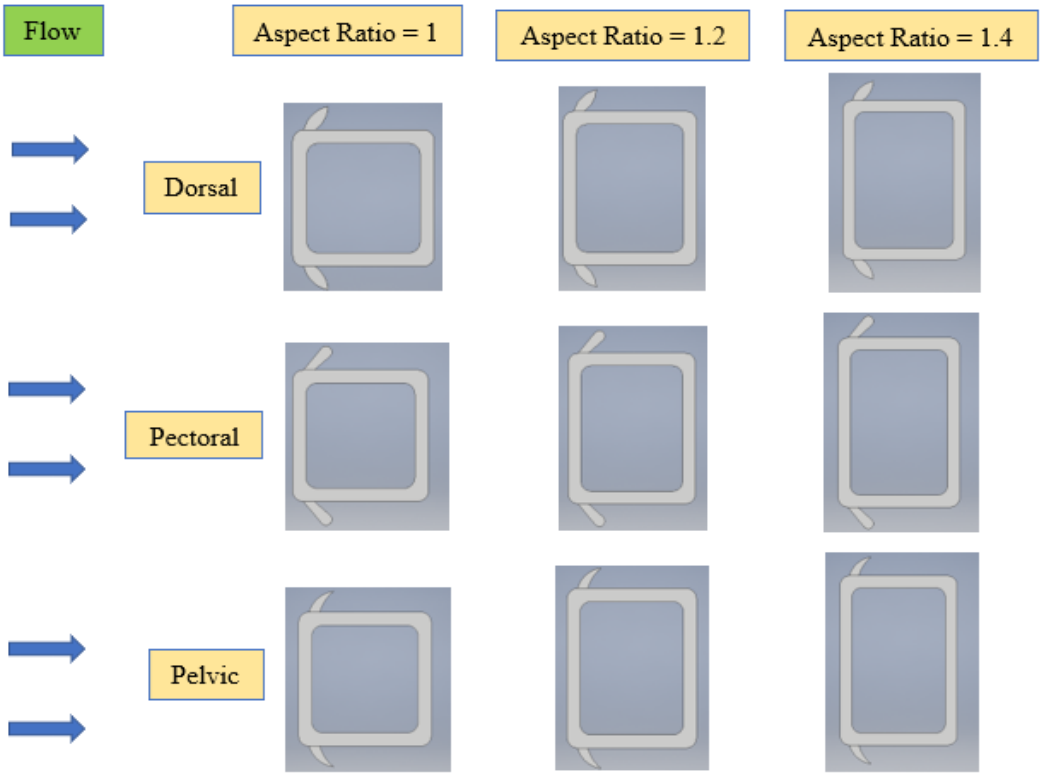

Figure 3.7. Combination of Rectangular Cylinders with Fins

A steel mounting/frame was attached on the top of the water tunnel to clamp the cylinders and the aluminum rod which was used to stick the flag. Both should be tight enough so no vibrations will be observed. In our study the blockage ratio was 6.25% and it was accepted according to Choi et al. [76]. Complete experimental setup is shown in Figure 3.8.

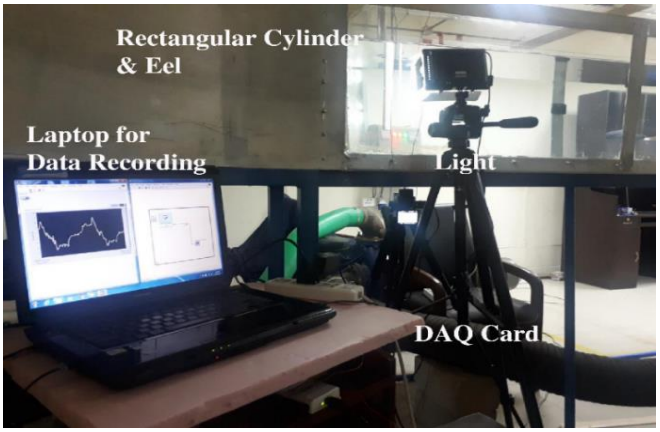

Figure 3.8. Complete experimental setup

In this experimental setup, the wire of the flag (which was water-proof) was connected with the bread board. On the bread board 1 mega-ohm resistor was connected and the other wire was attached to the DAQ (data acquisition) card which was NI-USB type 6009. Using a lab view software, voltage was recorded in PC.

Streamwise Gap (Gx) is defined as a distance from a center of a cylinder to the center of the eel/ flag in x-axis. In our case, the stream wise gap is between 1-4, which can be change by moving the flag position in horizontal direction (See Figure 3.9). LED light was attached on the side of the test area and the specification of LED is (Mcopus TTV 204). A pure black cloth was wrapped on the other side, so all the reflections will be prevented. A camera was placed at the bottom of the test area to observe the motion of the flag. Specification of the camera is Sony RX-100 IV. Our test area was transparent enough to observe all the activities of the flag using a camera.

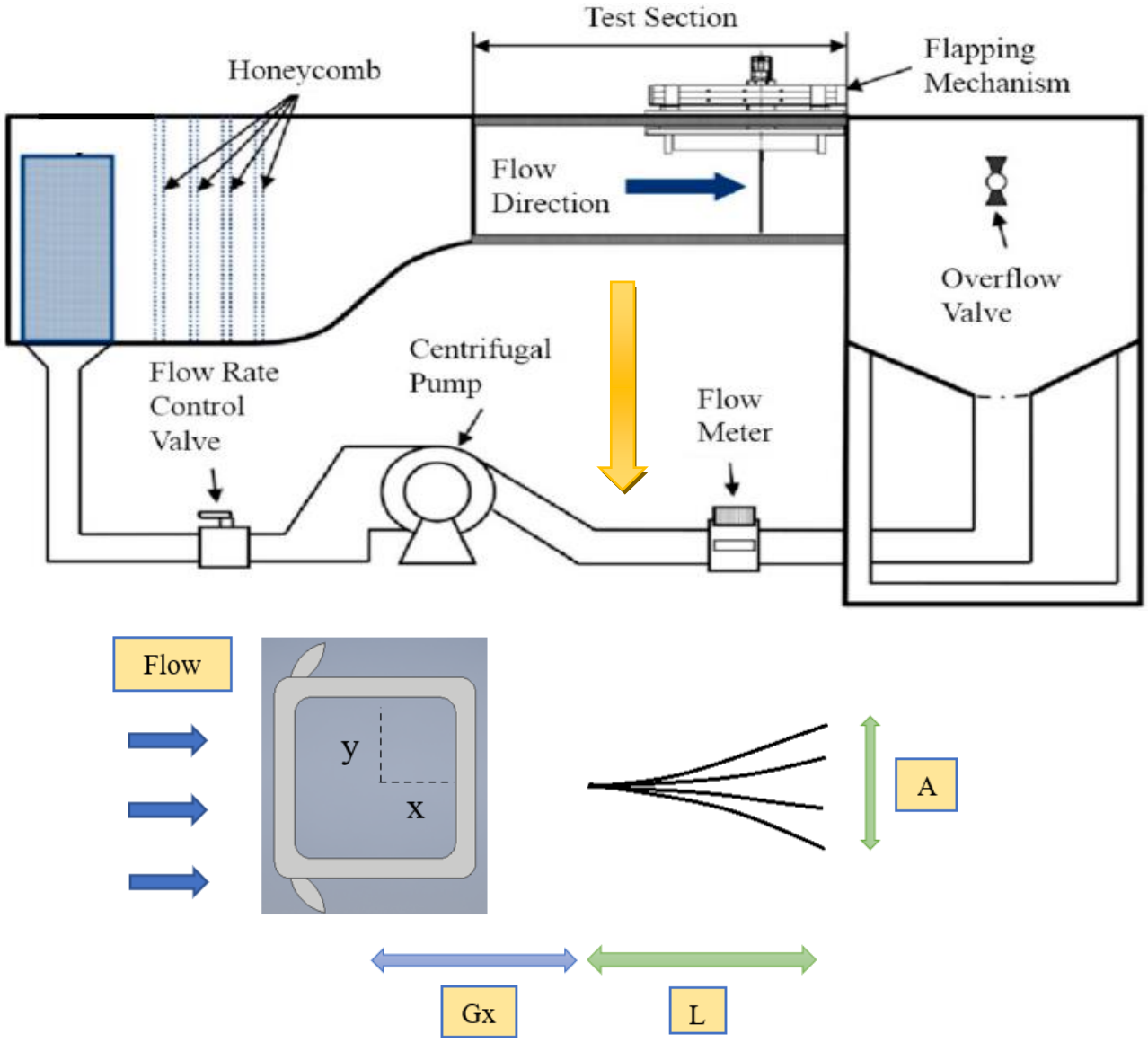

Figure 3.9. Schematic Diagram of Water Tunnel and Test Section

The trailing edge of the flag was free. When the water flows at a certain velocity strikes the bluff bodies, the water disperse and vortex was generated which allows the flag from trailing edge to oscillate at a required angle. More the vortex generated more the flag deflects from its original position. Camera at the bottom of the test sections record all the deflections. The duration of the video recorded by the camera is about 1-2 minutes. Then in post processing this video was run on the Matlab software which gives us the frequency and amplitude. By using these two factors, and the voltage which was calculated in each case by moving the flag at required streamwise gap, power can be calculated. The formula for calculating the power is:

$$P = \frac{V^2}{R}$$

V is the root mean square voltage and R is the resistance which is $1\text{M}\Omega$ Another Matlab code was run to split the video in different frames. Then we use all these frames to plot a graph using StarStax 0.71 software.

See table 3.2 for the complete description of the parameter used in our experimentation.

Parameter	Value
Cylinders Aspect Ratio (mm)	1, 1.2, 1.4
Cylinder wall thickness (*t*) (mm)	2.5
$Gx = g_x/D$	1 - 4
Blockage ratio	6.25 %
Velocity	0.26m/s
Reynold Number	3200
Flag active length (mm)	62
Density of flag (Kg/m^3)	1.78
Young's modulus	$2\text{-}4 \times 10^9$
Output voltage (V)	0.01 - 100
Impedance (MΩ)	1
Storage temperature (^{0}C)	-40 to +70
Operation temperature (^{0}C)	0 to +70

Table 3.2: Description of system's parameter.

Chapter 4

RESULT AND DISCUSSION

IMPACT OF RECTANGULAR BLUFFBODY HAVING FINS ON DYNAMICS OF FLAG BASED ENERGY HARVESTING

This research was based on the dynamic and performance of piezoelectric eel/flag which harvest energy by placing rectangular bluff bodies having fins in its wake. In this study we investigate rectangular bluff bodies with fins on its edges having different aspect ratio for distinct streamwise gap (Gx) between cylinder and the flag. Research shows that the frequency and amplitude was very important factors in obtaining the output power. By using bluff bodies of different aspect ratio, the wake was change. A hollow rectangular cylinder with fins having uniform flow was not studied yet. We can harvest energy by placing these cylinders at different gaps. In this study, we have compared all the 9 cylinders with each other and test which one will give higher output power. We have experimentally discussed each factor which has a great influence on the power like aspect ratio of cylinders, fins on cylinders, effect of velocity and streamwise gap between eel and cylinder. Our base case is circular cylinder having diameter of 25mm with 2.5mm thickness [77]. In this study, the velocity of the water in the tunnel was constant which was about 0.26m/s and the streamwise gap was between1-4. Using this velocity, we had calculated the Reynold number which was Re=3200. Total experimental cases in our study were 63. We can analyze each case and discover which fin or which cylinder will give higher output power or better performance. In the next section, we discuss in detail about the parameter used in the output power.

4.1 Parameters and fluid mechanics effecting flag energy harvesting:

When an eel or flag is placed in the wake of a bluff bodies (rectangular cylinder having fins) a strain is generated in it. Circular cylinder is taken as a base line case in our study. When rectangular cylinders are placed in the test section and water starts flowing, a kinetic energy is produces when the water strikes through the cylinders. Then this kinetic

energy will tend to oscillate the membrane which leads to the production of mechanical energy in the flag. Due to piezoelectric effect, the mechanical strain due to oscillation in the flag is then transformed into electrical energy.

A flapping is produced in the flag when the vortices produced by the cylinders strikes the flag. That flapping will create the electric energy. Some factors are responsible for the energy harvested by Piezoelectric eel like amplitude, frequency, capacitance of the eel layer and flag thickness etc. [78]. Two main factors on which the output power is dependent are oscillation amplitude and flapping frequency [79, 80]. The relation between power, flapping frequency 'f' and tip displacement 'y' is shown in this equation $P = y_t \times f^3$ [25]. By changing the aspect ratio of cylinders and by applying fins on the edges of the cylinder also effect the power output. Another equation which is used to calculate the harvested power is $P = V^2 / R$. 'V' is the voltage which is generated by the flapping of the piezoelectric membrane and record in the computer using the LabVIEW software and 'R' is the load resistance which is approximately 1MΩ. This is the optimum value of the resistance unless otherwise specified.

4.2 Effect of fins and aspect ratios of cylinders on energy harvesting:

4.2.1 Dorsal Fin:

a)

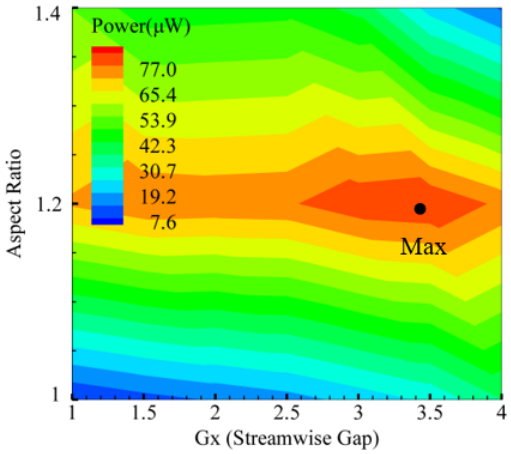

b)

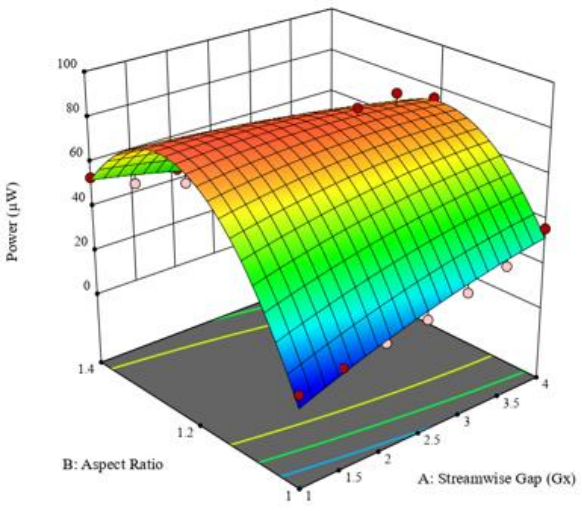

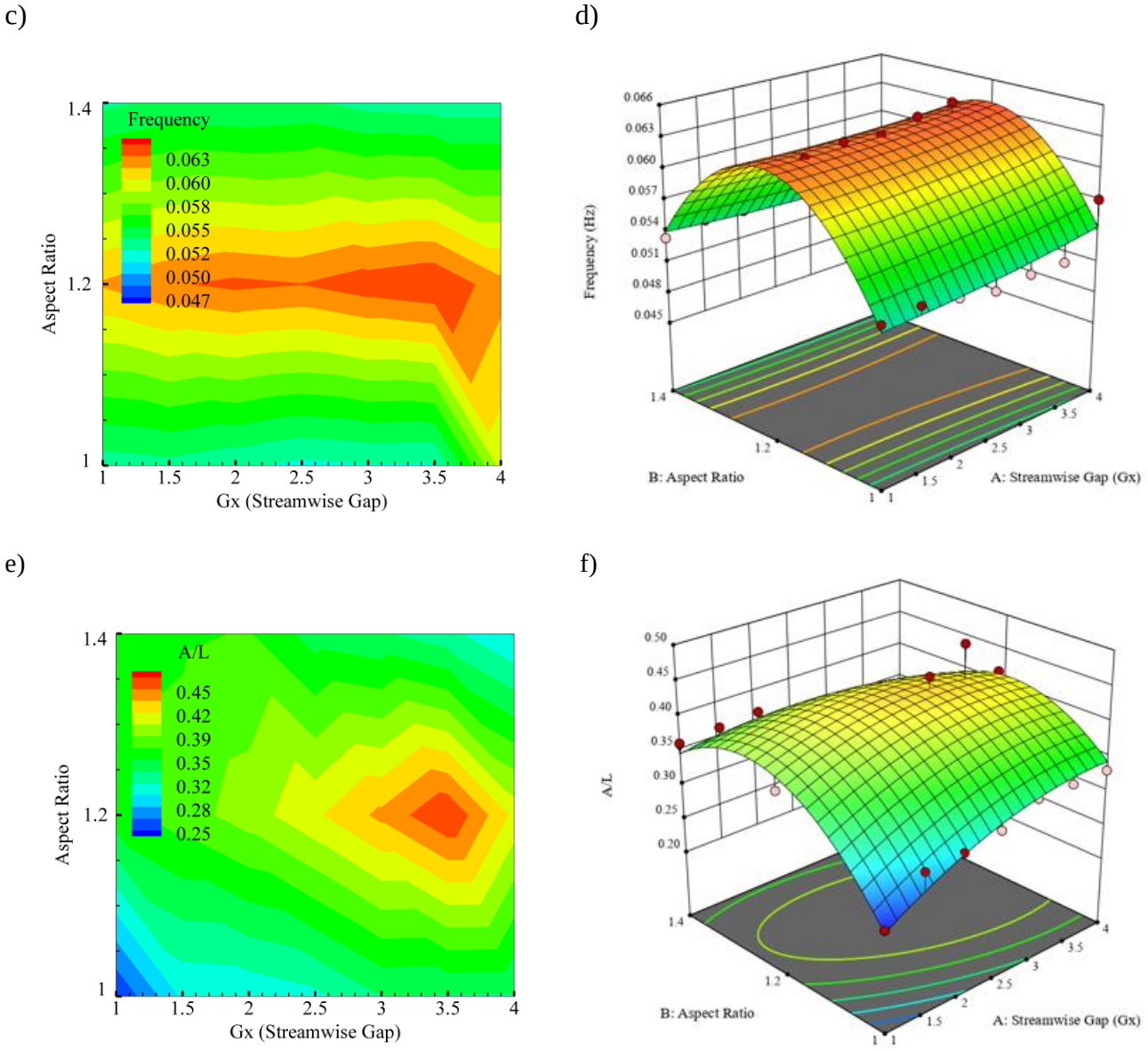

Figure 4.1. (a) 2D output power, (b) 3D output power, (c) 2D oscillating frequency, (d) 3D oscillating frequency (e) 2D flapping amplitude (*A/L*), (f) 3D flapping amplitude (*A/L*) at different aspect ratio and streamwise gap (Gx) for dorsal fins.

The effect of dorsal fin attached on the rectangular cylinders of different aspect ratios (A.R) and change of streamwise gap (Gx) on the output power, oscillating frequency and the flapping amplitude were discussed in Figure 4.1. All the 2D graphs were made on Tecplot software in which each detail of power, amplitude and frequency were prominently highlighted. Whereas all 3D graphs were made by using Design expert software. Figure 4.1(a, b) indicates that the maximum energy or power was harvested at streamwise gap (Gx) of 3.5 and at an aspect ratio of 1.2. In 2D graph highest power was indicated by 'Max' which is 82.74µW. 3D graph was also giving us the exact same contour which verifies the values. For rectangular cylinders having aspect ratio 1 and 1.4, the harvested power was minimum at

different Gx values. Now to understand the behavior of output power, oscillating frequency and flapping amplitude graphs needs to be discussed. Figure 4.1(c, d) shows the oscillation frequency at different stream wise gap. Higher frequency was observed in 1.2 aspect ratio rectangular cylinder at streamwise gap of $2 \leq Gx \leq 3.5$. At Gx 3.5, the frequency observed was 0.0645 due to which high strain was generated and cause high power. Whereas at other aspect ratio 1 and 1.4 low oscillation frequency was observed. Figure (e, f) indicated the flapping amplitude A/L at different Gx. 2D and 3D graphs shows that at Gx 3.5 and 1.2 aspect ratio A/L value was 0.472 higher than the other regions. Lower output power regions specially in aspect ratio 1 and 1.4 indicates the bad coupling of a wake with eel. So, no oscillation was produced in the membrane. Due to large oscillating frequency and amplitude at (Gx = 3.5 and 1.2 A.R) high strain was generated which results in maximum harvested power.

a)

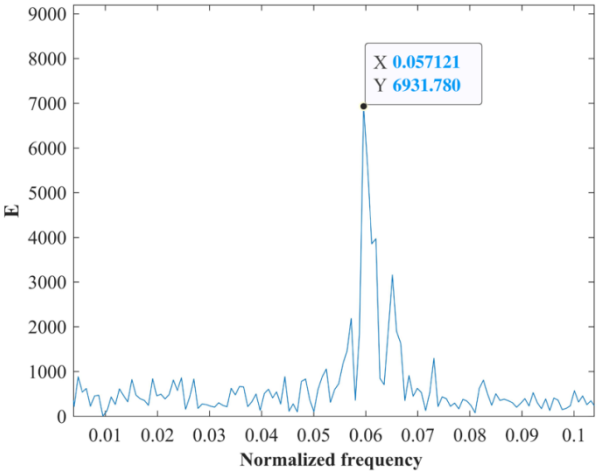

b)

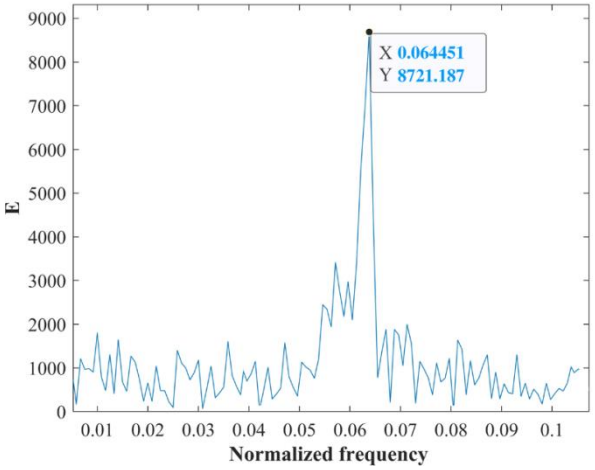

c)

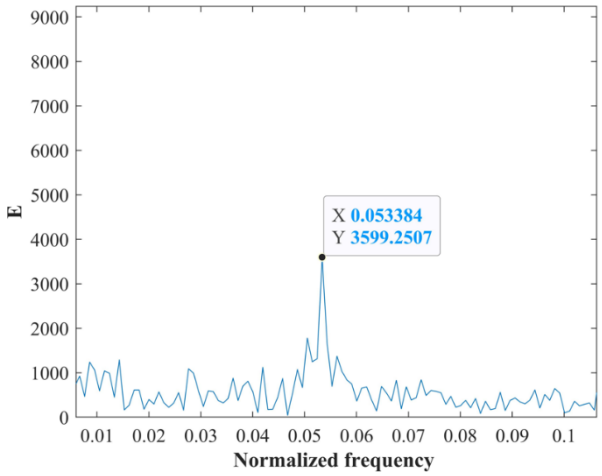

Figure 4.2. (a) Normalized Frequency at 1 A.R, (b) Normalized Frequency at 1.2 A.R, (c) Normalized Frequency at 1.4 A.R for dorsal fins

Figure 4.2 (a, b, c) indicates the normalized frequency w.r.t energy spectra at different aspect ratios. All these graphs were constructed on Matlab software. Figure 4.2 (a) denotes a normalized frequency graph at 1 aspect ratio rectangular cylinder with dorsal fins attached at the edges. It shows that the maximum frequency value is 0.0571. This maximum frequency had produced max strain which results in maximum power in that cylinder which was 36.39 µW at Gx = 4 see Figure 4.1 (a. b). Figure 4.2 (b) shows the frequency at 1.2 aspect ratio cylinder. Maximum frequency generated in this cylinder when dorsal fin attached was 0.0645 which generates maximum power output of 82.74µW at Gx = 3.5. Figure 4.2 (c) indicated maximum frequency region at 1.4 aspect ratio cylinder. In this case maximum value was 0.0534 which gives power of 53.60µW at Gx = 1. So, in dorsal fins having aspect ratio of 1.2 at Gx = 3.5, maximum frequency 0.0645 was generated which shows high strain value and good coupling of wake and membrane results in high power value of 82.74µW.

a) b)

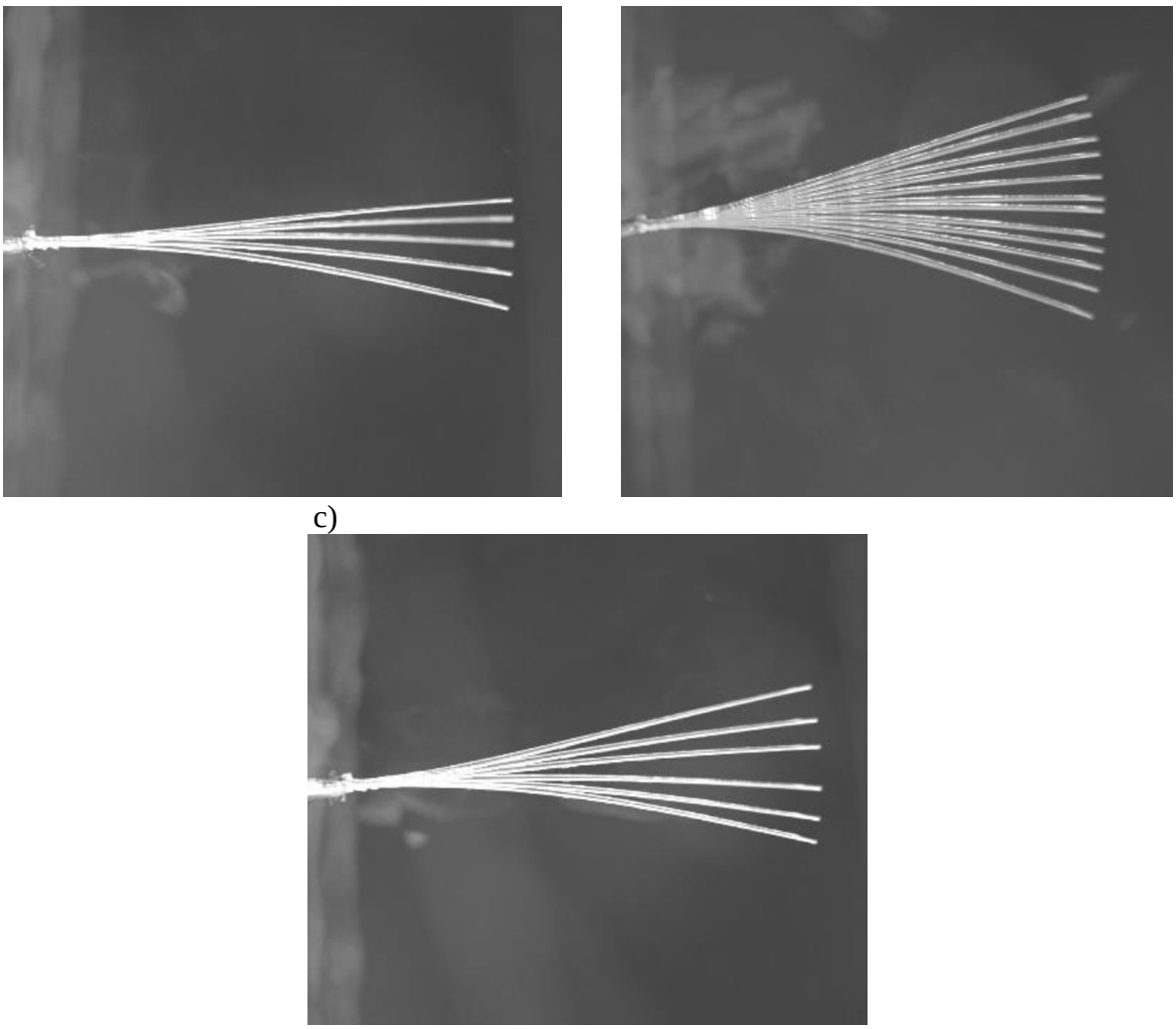

c)

Figure 4.3. Stroboscopic graph (a) Flapping amplitude at 1 A.R, (b) Flapping amplitude at 1.2 A.R, (c) Flapping amplitude at 1.4 A.R for dorsal fins.

Figure 4.3 indicates the flapping amplitude at the maximum power for all the rectangular cylinders. These graphs show the peak point on which high power was generated. In our study, the eel used was stiff having thickness of 0.188mm. Figure 4.3 (a) shows the flapping amplitude in 1 A.R rectangular cylinder. At a point when the power is maximum the A/L value is 0.331. These graphs were made using StarStax software. The value generated was same as shown in Figure 4.1 (e, f). In Figure 4.3 (b), the amplitude of 1.2 A.R rectangular cylinder was shown. At peak point the A/L value comes out to be 0.472. which is the maximum ones. Figure 4.3 (c) shows the flapping amplitude A/L at maximum energy harvesting pointy in 1.4 A.R rectangular cylinder. The value comes out at this point was 0.361. So, in the rectangular cylinder with dorsal fins attached at the edges having 1.2 aspect ratio gives the maximum A/L value of 0.472 at Gx = 3.5. Due to high flapping amplitude maximum power was produced. In this case large suction was observed at the bottom of the cylinder. Shear layer was pulled at the bottom of the cylinder and separates from the wake of cylinder, which results in maximum oscillation.

4.2.2 Pectoral Fin:

a)

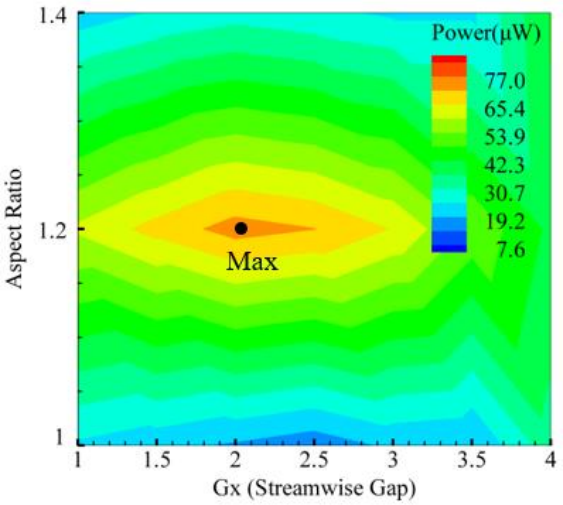

b)

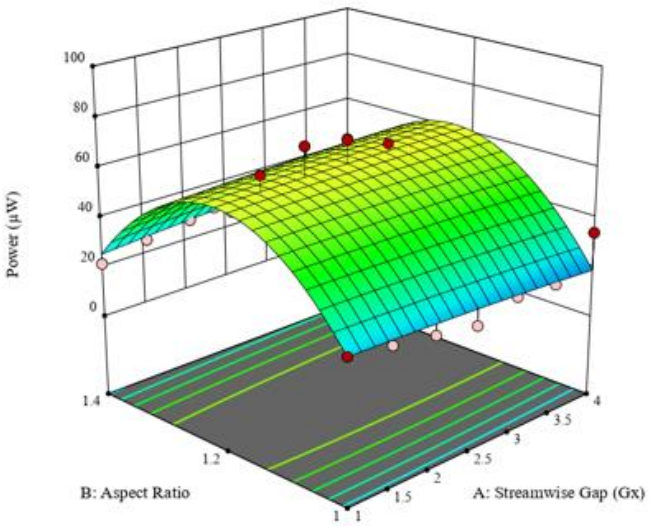

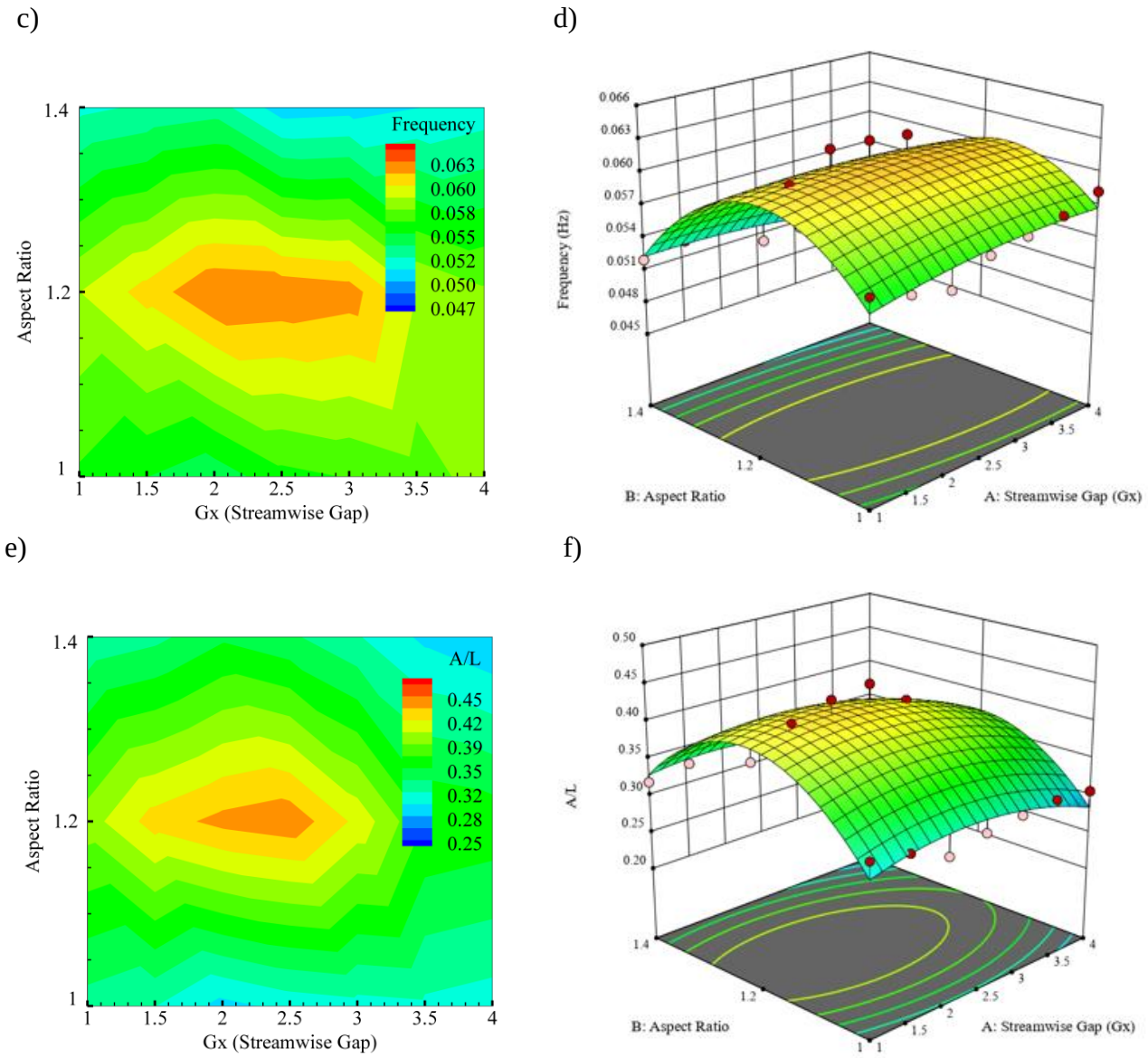

Figure 4.4. (a) 2D output power, (b) 3D output power, (c) 2D oscillating frequency, (d) 3D oscillating frequency (e) 2D flapping amplitude (*A/L*), (f) 3D flapping amplitude (*A/L*) at different aspect ratio and streamwise gap (Gx) for pectoral fins.

In Figure 4.4, we had discussed the effect of pectoral fin attached on the edges of rectangular cylinders having different aspect ratios (A.R) and change of streamwise gap (Gx) on the output power, frequency and the amplitude. Tecplot software was used to build up all 2D graphs and Design expert software was used for 3D graphs. Figure 4.4(a, b) indicates that the maximum power was harvested at streamwise gap (Gx) of 2 at 1.2 A.R rectangular cylinder. In 2D graph highest power was indicated by 'Max' which is 73.79µW. 3D graph was also gives us the exact same contour which verifies the values. For all type of fins, we have used the same contour levels so it may be helpful for better understanding in comparison. Low energy was harvested in case of 1 and 1.4 A.R rectangular cylinders on all

streamwise gaps (Gx).To analyze the behavior of harvested power, oscillating frequency and flapping amplitude graphs needs to be examined. Figure 4.4(c, d) shows the oscillation frequency at different stream wise gap. Higher frequency was observed in 1.2 A.R cylinder having streamwise gap of $1.5 \leq Gx \leq 3$. Maximum frequency was observed at Gx = 2 which was 0.0631 due to which high strain was generated and cause high output power. Whereas at 1 and 1.4 A.R, low oscillation frequency was observed. Figure (e, f) indicated the flapping amplitude A/L at different streamwise gaps. In this case maximum flapping amplitude was observed between $2 \leq Gx \leq 2.5$. The graphs show that at Gx = 2 and 1.2 aspect ratio, A/L value was 0.443 higher than the other A.R cylinders. Lower output power regions specially in aspect ratio 1 and 1.4 indicates the bad coupling of a wake with eel. So, no oscillation was produced in the membrane. Due to large oscillating frequency and amplitude at (Gx = 2 and 1.2 A.R) maximum harvested power was generated.

a) b)

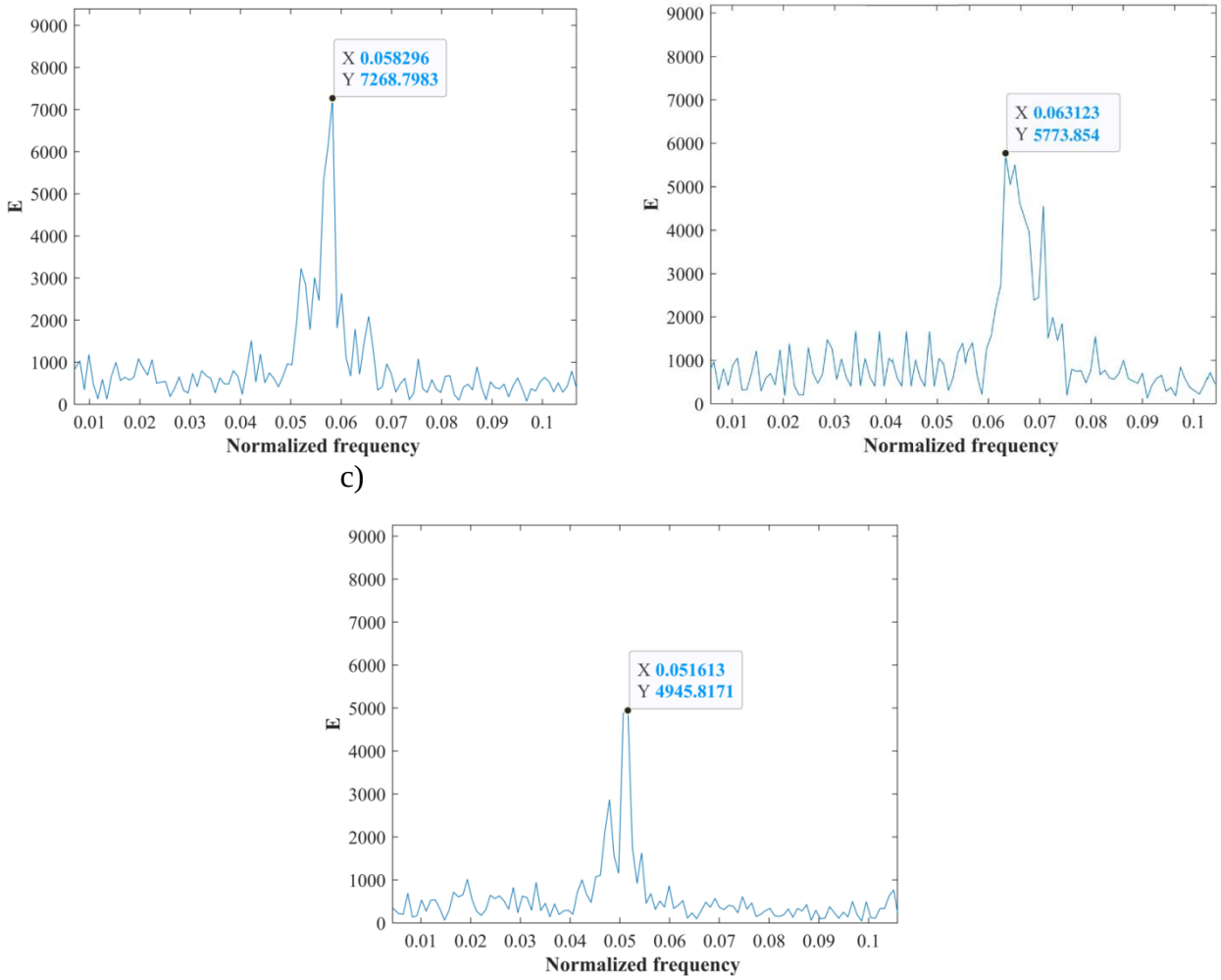

Figure 4.5. (a) Normalized Frequency at 1 A.R, (b) Normalized Frequency at 1.2 A.R, (c) Normalized Frequency at 1.4 A.R for pectoral fins.

Figure 4.5 (a, b, c) indicates the normalized frequency vs energy spectra at different aspect ratios. Matlab software was used to construct these frequency graphs. Figure 4.5 (a) shows that the normalized frequency graph at 1 A.R rectangular cylinder with pectoral fins attached at the edges. Maximum frequency observed in this case was 0.0583 having energy spectra of 7268.7. This maximum frequency had produced max strain which results in maximum power in that cylinder which was 34.27 µW at Gx = 4 see Figure 4.4 (a. b). Figure 4.5 (b) shows the frequency at 1.2 aspect ratio rectangular cylinder. Maximum frequency generated in this cylinder when pectoral fin attached was 0.0631 which generates maximum power output of 73.79µW at Gx = 2. This value is similar to the 2D and 3D graph shown in Figure 4.4 (c, d). Figure 4.5 (c) indicated maximum frequency region at 1.4 A.R cylinder. In this case maximum value was 0.0516 which gives power of 42.91µW at Gx = 4. Therefore, in pectoral fins having aspect ratio of 1.2 at Gx = 2, maximum frequency 0.0631 was generated which shows high strain value and good coupling of wake and membrane results in high power value of 73.79µW.

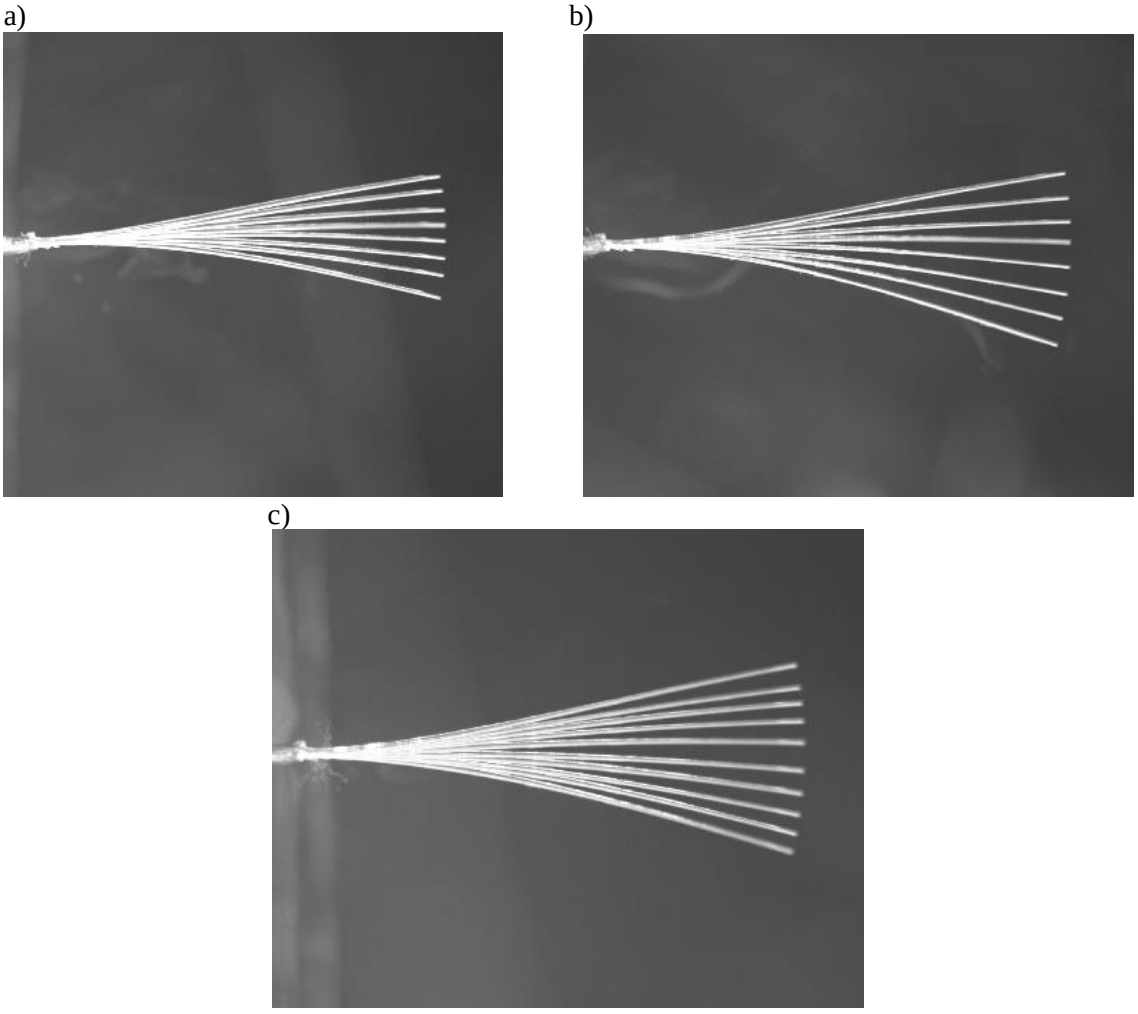

Figure 4.6. Stroboscopic graphs (a) Flapping amplitude at 1 A.R, (b) Flapping amplitude at 1.2 A.R, (c) Flapping amplitude at 1.4 A.R, for Pectoral fins.

Figure 4.6 indicates the flapping amplitude at the maximum power for all the rectangular cylinders. These stroboscopic graphs show the peak point on which high power was generated. Total 1 - 1.5min video was recorded from which these graphs can be extracted. Figure 4.6 (a) shows the flapping amplitude in 1 A.R rectangular cylinder. At a point when the power is maximum 34.27µW, the A/L value is 0.307. StarStax software was used to make these graphs. The value generated was same as shown in Figure 4.4 (e, f). In Figure 4.6 (b), the amplitude of 1.2 A.R rectangular cylinder was shown. At peak point of 73.79 µW the A/L value comes out to be 0.443. Figure 4.6 (c) shows the flapping amplitude A/L at maximum energy harvesting point of 42.91µW in 1.4 A.R rectangular cylinder. The value comes out at this point was 0.282. Therefore, in the rectangular cylinder with pectoral fins attached at the edges having 1.2 aspect ratio gives the maximum A/L value of 0.443 at Gx = 2. Due to high flapping amplitude maximum power of 73.79µW was produced. In this case large suction was observed at the bottom of the cylinder. Shear layer was pulled at the bottom of the cylinder and separates from the wake of cylinder, which results in maximum oscillation.

4.2.3 Pelvic Fin:

a)

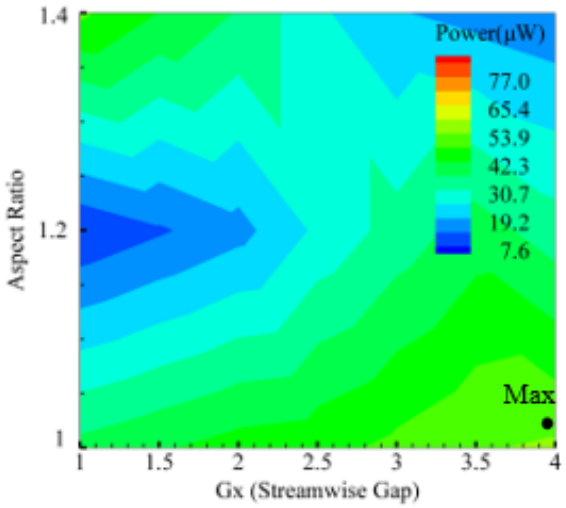

b)

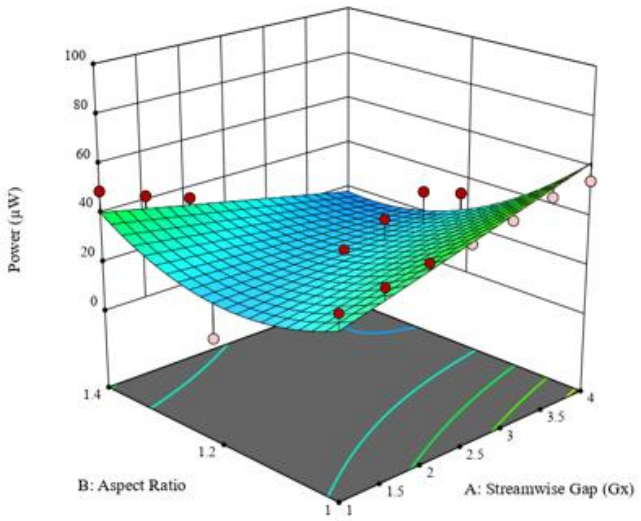

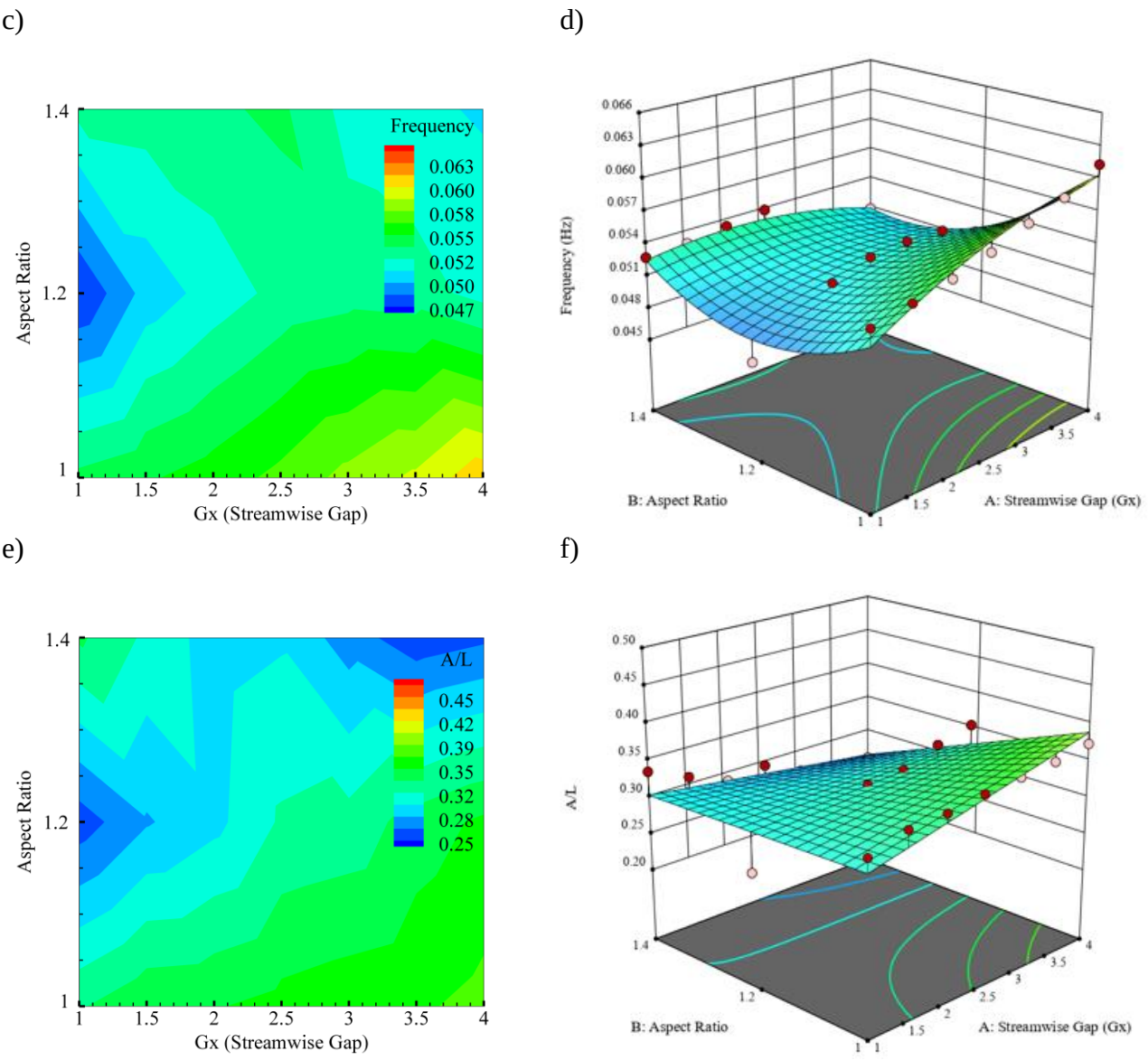

Figure 4.7. (a) 2D output power, (b) 3D output power, (c) 2D oscillating frequency, (d) 3D oscillating frequency (e) 2D flapping amplitude (*A/L*), (f) 3D flapping amplitude (*A/L*) at different aspect ratio and streamwise gap (Gx) for Pelvic fins.

In Figure 4.7, we had discussed the effect of pelvic fin attached on the edges of rectangular cylinders having different aspect ratios (A.R) and change of streamwise gap (Gx) on the output power, frequency and the amplitude. Figure 4.7 (a, b) indicates that the maximum power was harvested at streamwise gap (Gx) of 4 at 1 A.R rectangular cylinder. In 2D graph highest power was indicated by 'Max' which is 54.65µW. 3D graph was also gives us the exact same contour which verifies the values. Low energy was harvested in case of 1.2 and 1.4 A.R rectangular cylinders on all streamwise gaps (Gx). Figure 4.7 (c, d) shows the oscillation frequency at different stream wise gap. Higher frequency was observed in 1 A.R

cylinder at Gx = 4 which was 0.0614 due to which high strain was generated and cause high output power. Whereas at 1.2 and 1.4 A.R, low oscillation frequency was observed. Figure (e, f) indicated the flapping amplitude A/L at different streamwise gaps. In this case maximum flapping amplitude was observed at Gx = 4.and 1 A.R. A/L value was 0.373 higher than the other A.R cylinders. Lower output power regions especially in aspect ratio 1.2 and 1.4 indicates the bad coupling of a wake with eel. So, minimum oscillation was produced in the membrane. Due to large oscillating frequency and amplitude at (Gx = 4 and 1 A.R) maximum power

a)

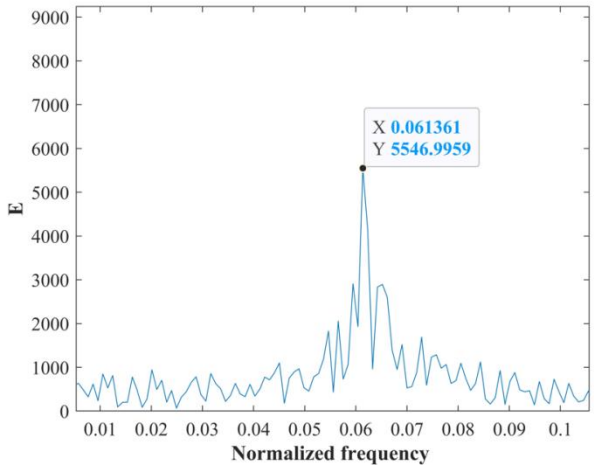

b)

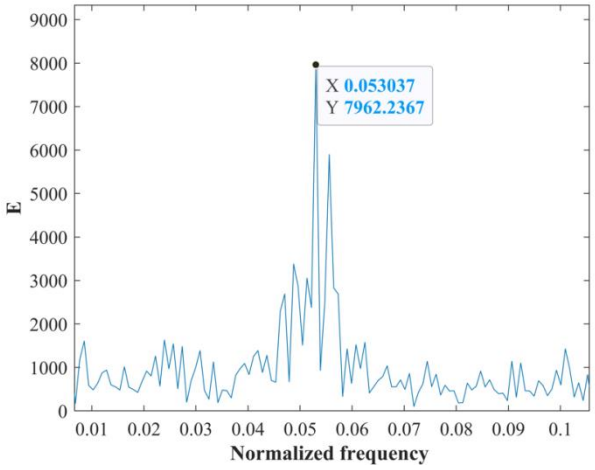

c)

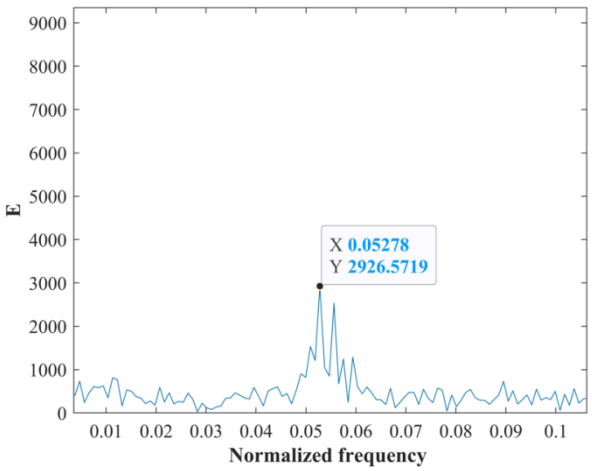

Figure 4.8 (a) Normalized Frequency at 1 A.R, (b) Normalized Frequency at 1.2 A.R, (c) Normalized Frequency at 1.4 A.R, for Pelvic fin

Figure 4.8 indicates the normalized frequency vs energy spectra at different aspect ratios. Figure 4.8 (a) shows that the normalized frequency graph at 1 A.R rectangular cylinder

with pelvic fins attached. Maximum frequency observed in this case was 0.0614 having energy spectra of 5546.9. This maximum frequency had produced max strain which results in maximum power in that cylinder which was 54.65μW at Gx = 4 see Figure 4.7 (a. b). Figure 4.8 (b) shows the frequency at 1.2 aspect ratio rectangular cylinder. Maximum frequency generated in this cylinder when pelvic fin attached was 0.0530 which generates maximum power output of 39.37μW at Gx = 3.5. This value is similar to the 2D and 3D graph shown in Figure 4.7 (c, d). Figure 4.5 (c) indicated maximum frequency region at 1.4 A.R cylinder. In this case maximum value was 0.0528 which gives power of 49.34μW at Gx = 1. Therefore, in pelvic fins having aspect ratio of 1 at Gx = 4, maximum frequency 0.0614 was generated which shows high strain value and good coupling of wake and membrane results in high power value of 54.65μW.

a)

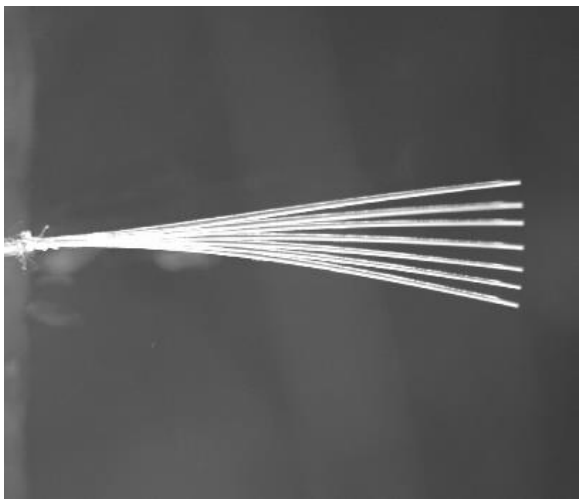

b)

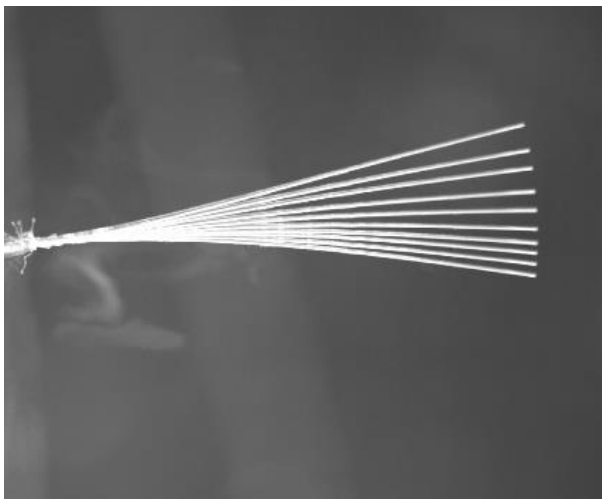

c)

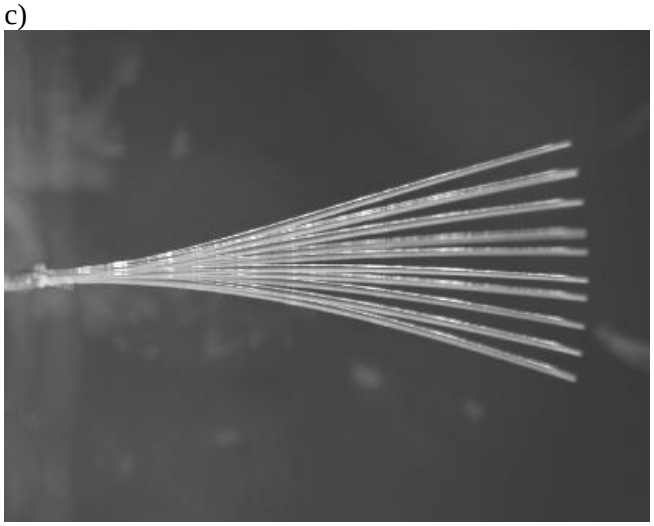

Figure 4.9. Stroboscopic graphs (a) Flapping amplitude at 1 A.R, (b) Flapping amplitude at 1.2 A.R, (c) Flapping amplitude at 1.4 A.R, for Pelvic fins.

Figure 4.9 shows that the flapping amplitude at the maximum power for all the rectangular cylinders. These stroboscopic graphs show the peak point on which high power was generated. Total 60 -70 sec video was recorded from which these graphs can be extracted. Figure 4.9 (a) shows the flapping amplitude in 1 A.R rectangular cylinder. At a point when the power is maximum 54.65µW, the A/L value is 0.373. The value generated was same as shown in Figure 4.7 (e, f). In Figure 4.9 (b), the amplitude of 1.2 A.R rectangular cylinder was shown. At peak point of 39.37µW the A/L value comes out to be 0.341. Figure 4.9 (c) shows the flapping amplitude A/L at maximum energy harvesting point of 49.34µW in 1.4 A.R rectangular cylinder. The value comes out at this point was 0.336. Therefore, in the rectangular cylinder with pelvic fins attached at the edges having 1 aspect ratio gives the maximum A/L value of 0.373 at Gx = 4. Due to high flapping amplitude maximum power of 54.65µW was produced. In this case large suction was observed at the bottom of the cylinder. Shear layer was pulled at the bottom of the cylinder and separates from the wake of cylinder, which results in maximum oscillation.

4.3 Overall Comparison Between Different Fins:

(a)

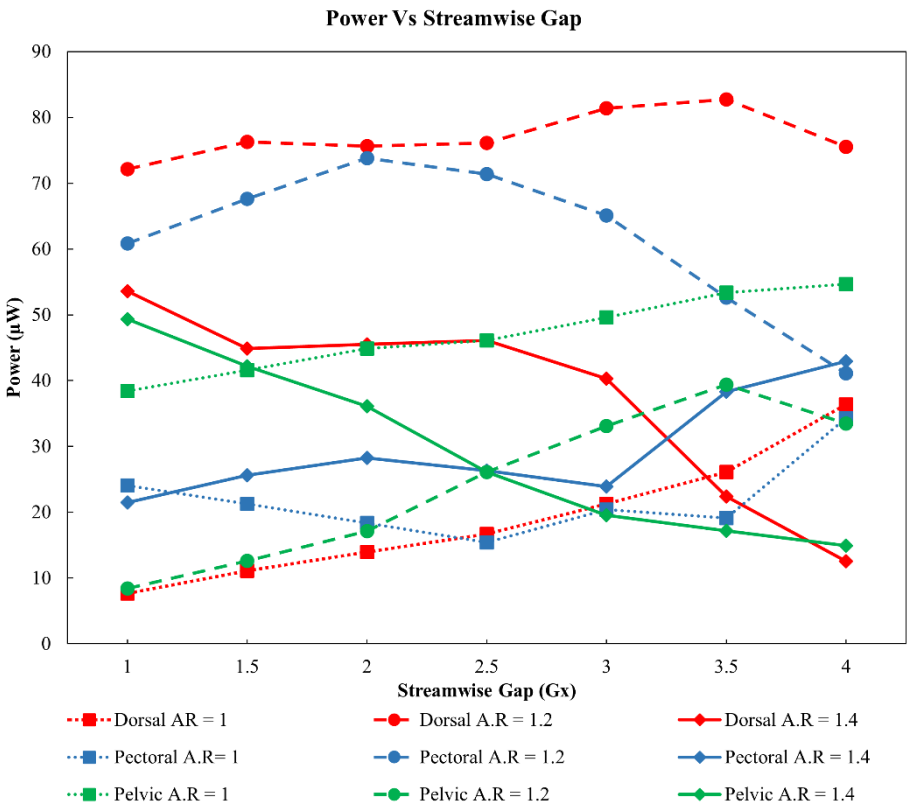

(b)

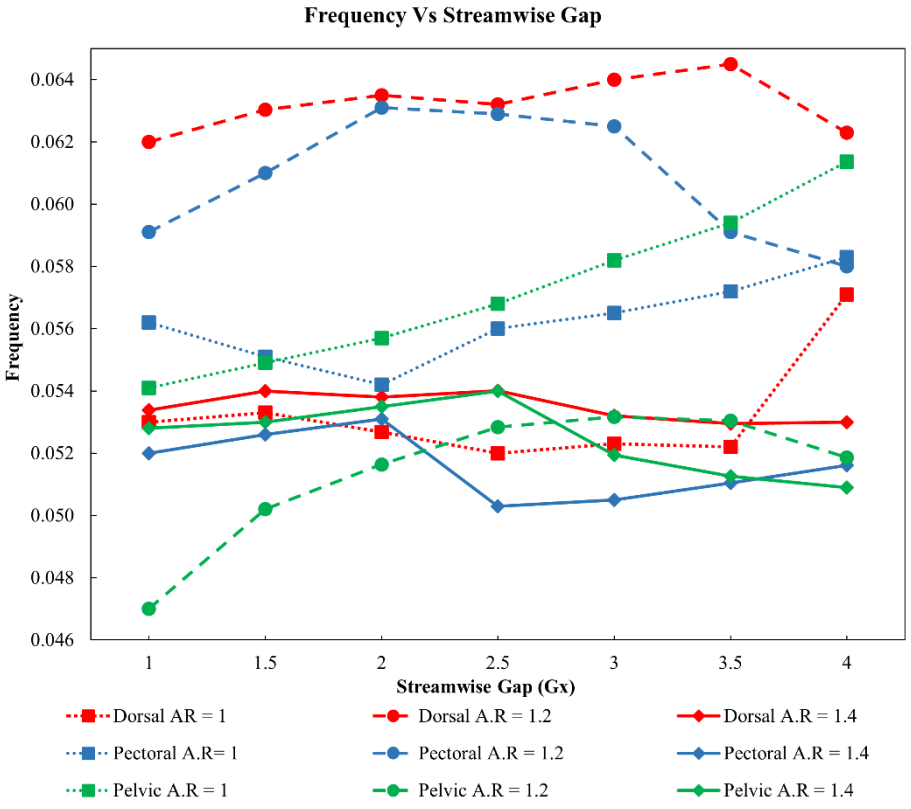

(c)

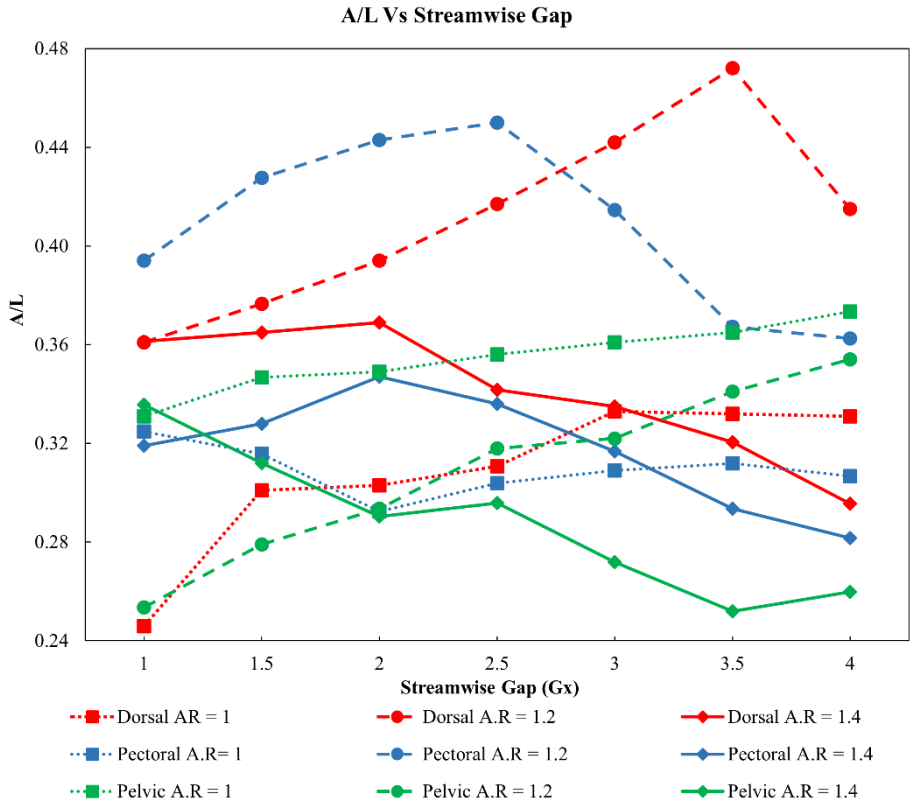

Figure 4.10. Overall comparison between each rectangular cylinders with fins (a) Power vs Streamwise gap (b) Frequency vs Streamwise gap (c) A/L vs Streamwise gap

Figure 4.10 shows the overall comparison between rectangular cylinders of different aspect ratio with three different types of fins (Dorsal, Pectoral and Pelvic) attached on the edges. Figure 4.10 (a) shows the output power at different streamwise gap (Gx) for each cylinder. By changing the streamwise gap between cylinder and flag at constant velocity of 0.257m/s power was fluctuating. Maximum power was achieved at Gx = 3.5 in Dorsal 1.2 A.R rectangular cylinder which is 82.74μW. Minimum power was shown in 1 A.R rectangular cylinder in Dorsal fin at Gx = 1 which is 7.63μW. In other streamwise gaps, the coupling of membrane with wake is minimum due to which low power was extracted. As Gx was increased further for 3.5 there was no further increase in power and the connection of a wake with the flag starts to break. After Dorsal 1.2 A.R cylinder, Pectoral fin with 1.2 aspect ratio rectangular cylinder gives better energy harvesting.

Figure 4.10 (b) indicates the frequency at different streamwise gap for each aspect ratio rectangular cylinder. Dorsal 1.2 A.R rectangular cylinder gives the maximum frequency of 0.0645Hz better than the other bluff bodies. Due to high frequency, large strain was produced which results in maximum output power. Minimum frequency was shown in 1 A.R cylinder in dorsal fin at Gx = 1. Minimum oscillation frequency is 0.047Hz. At this point the coupling of wake and flag is poor which results in minimum power.

Figure 4.10 (c) shows the comparison of A/L with different stream wise gap (Gx) for each fin attached on the cylinder. It indicates that the 1.2 A.R cylinder with dorsal fin attached at the edges had given maximum A/L value than all the other cylinders. At Gx = 3.5 the A/L value is 0.472. After dorsal fin, pectoral fin with 1.2 A.R cylinder had given better performance at Gx = 2.5. Lowest A/L value was indicated at Gx = 1 in dorsal fin with 1 A.R rectangular cylinder. Lowest value was 0.246.

Overall comparison shows that the dorsal fin attached on 1.2 aspect ratio rectangular cylinder gives maximum harvesting power, due to high oscillating frequency and flapping amplitude which produce high strain. Table 4.1 shows the value which was obtained during experimentation in each cylinder. In this table each cylinder values is written in each fin.

(a)

Cylinder Shape	Fin Type	Distance form Center of Cylinder to Eel in X-Axis (S, mm)	Gx = S/D	Power (μW)	Frequency	A/L
Rectangular (A.R = 1)	Dorsal	25	1	7.63	0.0470	0.246
		37.5	1.5	11.10	0.0533	0.301
		50	2	13.94	0.0527	0.303
		62.5	2.5	16.68	0.0520	0.311
		75	3	21.24	0.0523	0.333
		87.5	3.5	26.10	0.0522	0.332
		100	4	36.39	0.0571	0.331
	Pectoral	25	1	24.03	0.0562	0.325
		37.5	1.5	21.26	0.0551	0.316
		50	2	18.35	0.0542	0.292
		62.5	2.5	15.41	0.0560	0.304
		75	3	20.38	0.0565	0.309
		87.5	3.5	19.10	0.0572	0.312
		100	4	34.27	0.0583	0.307
	Pelvic	25	1	38.40	0.0541	0.331
		37.5	1.5	41.60	0.0549	0.347
		50	2	44.85	0.0557	0.349
		62.5	2.5	46.10	0.0568	0.356
		75	3	49.60	0.0582	0.361
		87.5	3.5	53.34	0.0594	0.365
		100	4	54.65	0.0614	0.373

(b)

Cylinder Shape	Fin Type	Distance form Center of Cylinder to Eel in X-Axis (S, mm)	Gx = S/D	Power (μW)	Frequency	A/L
Rectangular (A.R = 1.2)	Dorsal	30	1	72.14	0.0620	0.361
		45	1.5	76.27	0.0630	0.377
		60	2	75.60	0.0635	0.394
		75	2.5	76.10	0.0632	0.417
		90	3	81.40	0.0640	0.442
		105	3.5	82.74	0.0645	0.472
		120	4	75.50	0.0623	0.415
	Pectoral	30	1	60.83	0.0591	0.394
		45	1.5	67.62	0.0610	0.428
		60	2	73.79	0.0631	0.443
		75	2.5	71.38	0.0629	0.450
		90	3	65.08	0.0625	0.415
		105	3.5	52.60	0.0591	0.367
		120	4	41.10	0.0580	0.362
		30	1	8.40	0.0530	0.254
		45	1.5	12.60	0.0502	0.279

	Pelvic	60	2	17.10	0.0516	0.293
		75	2.5	26.10	0.0528	0.318
		90	3	33.10	0.0532	0.322
		105	3.5	39.37	0.0530	0.341
		120	4	33.48	0.0519	0.354

(c)

Cylinder Shape	Fin Type	Distance form Center of Cylinder to Eel in X-Axis (S, mm)	Gx = S/D	Power (µW)	Frequency	A/L
Rectangular (A.R=1.4)	**Dorsal**	35	1	53.60	0.0534	0.361
		52.5	1.5	44.89	0.0540	0.365
		70	2	45.53	0.0538	0.369
		87.5	2.5	46.10	0.0540	0.342
		105	3	40.27	0.0532	0.335
		122.5	3.5	22.39	0.0530	0.321
		140	4	12.54	0.0530	0.296
	Pectoral	35	1	21.49	0.0520	0.319
		52.5	1.5	25.60	0.0526	0.328
		70	2	28.27	0.0531	0.347
		87.5	2.5	26.30	0.0503	0.336
		105	3	23.90	0.0505	0.317
		122.5	3.5	38.28	0.0510	0.294
		140	4	42.91	0.0516	0.282
	Pelvic	35	1	49.34	0.0528	0.336
		52.5	1.5	42.20	0.0530	0.312
		70	2	36.10	0.0535	0.290
		87.5	2.5	26.10	0.0540	0.296
		105	3	19.56	0.0519	0.272
		122.5	3.5	17.15	0.0513	0.252
		140	4	14.89	0.0509	0.260

Table 4.1 Values obtained during experimentation across each rectangular cylinder

(a) Rectangular cylinder (1 A.R) with Dorsal, Pectoral and Pelvic fins

(b) Rectangular cylinder (1.2 A.R) with Dorsal, Pectoral and Pelvic fins

(c) Rectangular cylinder (1.4 A.R) with Dorsal, Pectoral and Pelvic fins.

4.4 Comparison with Baseline Case:

In this section, we were comparing our experimental values with our baseline case. Our baseline case was hollow circular cylinder. Table 4.2 was taken from the other research in which solid, hollow and other inverted circular cylinders were experimentally studied. This table shows that the maximum value was obtained by used inverted hollow circular cylinder at the velocity of 0.26m/s. In section 4.3, we have discussed in detail using graphs and tables about our experimental values which were obtained at a constant velocity of 0.26m/s having different types of fins (Dorsal, Pectoral and Pelvic) attached on the rectangular cylinder of different aspect ratios. We concluded that by using dorsal fin attached on the 1.2 aspect ratio rectangular cylinder had given maximum power of 82.74μW better than the solid, hollow and inverted circular cylinders. This value was obtained at the streamwise gap of Gx = 3.5. Due to high oscillating frequency and high flapping amplitude, high strain was generated which results in high power. If we will compare the inverted hollow cylinder with our study, 5% more power was harvested.

Cross Section	**Maxima**	***U*(m/s)**	**Harvested power (μW)**
Solid C	*Mx*	0.26	57.91
Hollow C	*Mx*	0.26	63.99
Inverted Solid C	*Mx*	0.26	63.59
Inverted Hollow C	*Mx*	0.26	78.13

Table 4.2 Comparison of different bluff bodies with maximum power [77]

Chapter 5

CONCLUDING REMARKS

5.1 Conclusion

In our study, we had discussed the energy harvesting by using bio inspired fins like Dorsal, Pectoral and Pelvic on rectangular cylinders of different aspect ratio. We had performed the experiment at the constant velocity of 0.26m/s and changed the streamwise gap (Gx) to get maximum output power.

In this study we have analyzed different factors or parameters which was affecting the energy harvesting system. The important parameters which generated great impact on output power are cross sectional area of bluff bodies, velocity, bio inspired fins, streamwise gap (Gx) and stiffness of the flag. This was an easy method to extra the natural energy.

In 4^{th} chapter, we had discussed detail experimental study in which we had used 3 different types of rectangular cylinders with 3 types of fins attached on the edges which comes out to be total 9 cylinders on which experiments were done. Dorsal fin has given us the better results than other fins. When dorsal fin was attached on the 1.2 A.R rectangular cylinder it has given us maximum energy harvesting. High strain was generated when this cylinder was placed at the stream wise gap of 3.5 due to which high oscillation frequency and flapping amplitude was observed which results in maximum power output. After dorsal fin pectoral fin was showing us good results.

Streamwise gap is varied from 1 to 4. By changing the streamwise gap between cylinder and flag the output power changes. Experimentally we had analyzed that between $2 \leq Gx \leq 3.5$ coupling of wake and the flag was good and it had generated some power. But at $Gx = 3.5$ we had extracted maximum power by using 1.2 aspect ratio rectangular cylinder. After $Gx = 3.5$ power start dropping.

In section 4.3 and 4.4 we had compared all the experimental results and found out which cylinder or which fins has given us better energy harvesting. Also, we had compared our values with the base line case which was hollow circular cylinder. By changing the streamwise gap between cylinder and flag at constant velocity of 0.26m/s power was fluctuating. Maximum power was achieved at $Gx = 3.5$ in Dorsal 1.2 A.R rectangular cylinder which is 82.74μW. Minimum power was shown in 1 A.R rectangular cylinder in Dorsal fin at $Gx = 1$ which is 7.63μW. If we had compared the hollow circular cylinder with

our study, 5-10% more power was harvested.

5.2 Future Recommendation

In our study, we had tried a lot to go in detail and discuss every aspect how we can achieve more energy harvesting but still there is a lot of potential in this research and someone will proceed this research by putting some extra idea. For future work some recommendations are proposed:

- Detail simulation work and PIV needs be performed by using these rectangular cylinders.

- Field of biomimetic needs to be further study and will use other types of fins to extract more output power.

- To apply this research in real environment, like in the oceans, small rivers, cool and hot environment so the bigger image will be seen about how much more energy can be harvested.

- There is a need to work on lift and drag coefficients for different shapes and discuss various parameters and properties of wake.

- Shedding Frequency can be measured by using hot wire anemometry test.

- This study is a small-scale model which was experimentally studied in lab. Need to work on large scale model in industry or in real environment with more parameters used to get more optimal results.

REFERENCES

1. Sudevalayam, S. and P. Kulkarni, *Energy harvesting sensor nodes: Survey and implications.* IEEE communications surveys & tutorials, 2010. **13**(3): p. 443-461.
2. Priya, S., *Advances in energy harvesting using low profile piezoelectric transducers.* Journal of electroceramics, 2007. **19**(1): p. 167-184.
3. Gungor, V.C. and G.P. Hancke, *Industrial wireless sensor networks: Challenges, design principles, and technical approaches.* IEEE Transactions on industrial electronics, 2009. **56**(10): p. 4258-4265.
4. Tan, Y.K. and S.K. Panda, *Energy harvesting from hybrid indoor ambient light and thermal energy sources for enhanced performance of wireless sensor nodes.* IEEE Transactions on Industrial Electronics, 2010. **58**(9): p. 4424-4435.
5. Basagni, S., et al., *Wireless Sensor Networks with Energy Harvesting.* Mobile ad hoc networking, 2013. **1**: p. 701-736.
6. Ang, R., Y. Tan, and S. Panda. *Energy harvesting for autonomous wind sensor in remote area*. in *IECON 2007-33rd Annual Conference of the IEEE Industrial Electronics Society*. 2007. IEEE.
7. Glynne-Jones, P., et al., *An electromagnetic, vibration-powered generator for intelligent sensor systems.* Sensors and Actuators A: Physical, 2004. **110**(1-3): p. 344-349.
8. Vullers, R., et al., *Micropower energy harvesting.* Solid-State Electronics, 2009. **53**(7): p. 684-693.
9. Adnan Harb, *Energy harvesting: State-of-the-art. Renewable Energy,.* ELSEVIER, 2011. **36**(10): p. 2641-2654.
10. Shepherd, D.G. *Historical development of the windmill*. 1990.
11. Stefano Olivieri, G.B., Andrea Mazzino, Corrado Boragno,, *FLuttering Energy Harvester for Autonomous Powering (FLEHAP): aeroelastic characterisation and preliminary performance evaluation, Procedia Engineering.* ELSEVIER, 2017. **199**: p. 3474-3479.
12. Boragno, C., R. Festa, and A. Mazzino, *Elastically bounded flapping wing for energy harvesting.* Applied Physics Letters, 2012. **100**(25): p. 253906.
13. Zhu, Q., *Energy harvesting by a purely passive flapping foil from shear flows.* Journal of fluids and structures, 2012. **34**: p. 157-169.
14. *The Piezoelectric Effect - Piezoelectric Motors & Motion Systems*. n.d.
15. Walter Heywang, K.L., Wolfram Wersing, *Piezoelectricity : evolution and future of a*

technology. 2008.

16. Ramadan, K.S., D. Sameoto, and S. Evoy, *A review of piezoelectric polymers as functional materials for electromechanical transducers.* Smart Materials and Structures, 2014. **23**(3): p. 033001.
17. Tang, L., M.P. Païdoussis, and J. Jiang, *Cantilevered flexible plates in axial flow: energy transfer and the concept of flutter-mill.* Journal of Sound and Vibration, 2009. **326**(1-2): p. 263-276.
18. J.J. ALLEN, A.J.S., *ENERGY HARVESTING EEL,*. ELSEVIER, 2001. **15**(3-4): p. 629-640.
19. Singh, K., S. Michelin, and E. De Langre, *Energy harvesting from axial fluid-elastic instabilities of a cylinder.* Journal of Fluids and Structures, 2012. **30**: p. 159-172.
20. Dunnmon, J., et al., *Power extraction from aeroelastic limit cycle oscillations.* Journal of fluids and structures, 2011. **27**(8): p. 1182-1198.
21. Young, D.T.A.a.Y.L., *Hydroelastic response and energy harvesting potential of flexible piezoelectric beams in viscous flow.* Physics of Fluids 2012. **24**.
22. Barrero-Gil, A., G. Alonso, and A. Sanz-Andres, *Energy harvesting from transverse galloping.* Journal of Sound and Vibration, 2010. **329**(14): p. 2873-2883.
23. Karim, M.E., et al., *Energy Revolution for Our Common Future: An Evaluation of the Emerging International Renewable Energy Law.* Energies, 2018. **11**(7): p. 1769.
24. Iqbal, M. and F.U. Khan, *Hybrid vibration and wind energy harvesting using combined piezoelectric and electromagnetic conversion for bridge health monitoring applications.* Energy conversion and management, 2018. **172**: p. 611-618.
25. Mitcheson, P.D., et al., *Energy harvesting from human and machine motion for wireless electronic devices.* Proceedings of the IEEE, 2008. **96**(9): p. 1457-1486.
26. Ottman, G.K., et al., *Adaptive piezoelectric energy harvesting circuit for wireless remote power supply.* IEEE Transactions on power electronics, 2002. **17**(5): p. 669-676.
27. Usman, M., et al., *Experimental validation of a novel piezoelectric energy harvesting system employing wake galloping phenomenon for a broad wind spectrum.* Energy, 2018. **153**: p. 882-889.
28. Sultana, A., et al., *A pyroelectric generator as a self-powered temperature sensor for sustainable thermal energy harvesting from waste heat and human body heat.* Applied Energy, 2018. **221**: p. 299-307.
29. Song, G.J., et al., *Development of a pavement block piezoelectric energy harvester for self-powered walkway applications.* Applied Energy, 2019. **256**: p. 113916.

30. Wang, C., et al., *Optimization design and experimental investigation of piezoelectric energy harvesting devices for pavement.* Applied energy, 2018. **229**: p. 18-30.
31. Izadgoshasb, I., et al., *Optimizing orientation of piezoelectric cantilever beam for harvesting energy from human walking.* Energy conversion and management, 2018. **161**: p. 66-73.
32. Orrego, S., et al., *Harvesting ambient wind energy with an inverted piezoelectric flag.* Applied energy, 2017. **194**: p. 212-222.
33. Lallart, M., S. Pruvost, and D. Guyomar, *Electrostatic energy harvesting enhancement using variable equivalent permittivity.* Physics Letters A, 2011. **375**(45): p. 3921-3924.
34. Beeby, S.P., et al., *A micro electromagnetic generator for vibration energy harvesting.* Journal of Micromechanics and microengineering, 2007. **17**(7): p. 1257.
35. Hamlehdar, M., A. Kasaeian, and M.R. Safaei, *Energy harvesting from fluid flow using piezoelectrics: A critical review.* Renewable Energy, 2019. **143**: p. 1826-1838.
36. Maamer, B., et al., *A review on design improvements and techniques for mechanical energy harvesting using piezoelectric and electromagnetic schemes.* Energy Conversion and Management, 2019. **199**: p. 111973.
37. Kusch-Brandt, *Renewables 2019 Global Status Report*. 2019.
38. Naudascher, E. and D. Rockwell, *Flow-Induced Vibrations: An Engineering Guide*. 2017: Routledge.
39. Kim, H., S. Kang, and D. Kim, *Dynamics of a flag behind a bluff body.* Journal of Fluids and Structures, 2017. **71**: p. 1-14.
40. Silva-Leon, J., et al., *Simultaneous wind and solar energy harvesting with inverted flags.* Applied Energy, 2019. **239**: p. 846-858.
41. Wang, J., et al., *The state-of-the-art review on energy harvesting from flow-induced vibrations.* Applied Energy, 2020. **267**: p. 114902.
42. Akaydin, H.D., N. Elvin, and Y. Andreopoulos, *Energy harvesting from highly unsteady fluid flows using piezoelectric materials.* Journal of Intelligent Material Systems and Structures, 2010. **21**(13): p. 1263-1278.
43. Goushcha, O., N. Elvin, and Y. Andreopoulos, *Interactions of vortices with a flexible beam with applications in fluidic energy harvesting.* Applied Physics Letters, 2014. **104**(2): p. 021919.
44. Hu, Y., et al., *Modeling and experimental study of a piezoelectric energy harvester from vortex shedding-induced vibration.* Energy conversion and management, 2018. **162**: p. 145-158.

45. Pan, F., et al., *Designed simulation and experiment of a piezoelectric energy harvesting system based on vortex-induced vibration.* IEEE Transactions on Industry Applications, 2017. **53**(4): p. 3890-3897.
46. Wang, J., et al., *Hybrid wind energy scavenging by coupling vortex-induced vibrations and galloping.* Energy Conversion and Management, 2020. **213**: p. 112835.
47. Sun, W. and J. Seok, *A novel self-tuning wind energy harvester with a slidable bluff body using vortex-induced vibration.* Energy Conversion and Management, 2020. **205**: p. 112472.
48. Narendran, K., K. Murali, and V. Sundar, *Investigations into efficiency of vortex induced vibration hydro-kinetic energy device.* Energy, 2016. **109**: p. 224-235.
49. Hobbs, W.B. and D.L. Hu, *Tree-inspired piezoelectric energy harvesting.* Journal of fluids and Structures, 2012. **28**: p. 103-114.
50. Zhao, L.-C., et al., *Magnetic coupling and flextensional amplification mechanisms for high-robustness ambient wind energy harvesting.* Energy Conversion and Management, 2019. **201**: p. 112166.
51. Zhang, L., et al., *Experimental investigation of aerodynamic energy harvester with different interference cylinder cross-sections.* Energy, 2019. **167**: p. 970-981.
52. Shan, X., et al., *Energy-harvesting performances of two tandem piezoelectric energy harvesters with cylinders in water.* Applied Sciences, 2016. **6**(8): p. 230.
53. Abdelkefi, A., et al., *Performance enhancement of piezoelectric energy harvesters from wake galloping.* Applied Physics Letters, 2013. **103**(3): p. 033903.
54. Akaydin, H., N. Elvin, and Y. Andreopoulos, *The performance of a self-excited fluidic energy harvester.* Smart materials and Structures, 2012. **21**(2): p. 025007.
55. Dai, H., A. Abdelkefi, and L. Wang, *Theoretical modeling and nonlinear analysis of piezoelectric energy harvesting from vortex-induced vibrations.* Journal of Intelligent Material Systems and Structures, 2014. **25**(14): p. 1861-1874.
56. Rezaei, M. and R. Talebitooti, *Wideband PZT energy harvesting from the wake of a bluff body in varying flow speeds.* International Journal of Mechanical Sciences, 2019. **163**: p. 105135.
57. Zhao, L., L. Tang, and Y. Yang, *Comparison of modeling methods and parametric study for a piezoelectric wind energy harvester.* Smart materials and Structures, 2013. **22**(12): p. 125003.
58. He, X., X. Yang, and S. Jiang, *Enhancement of wind energy harvesting by interaction between vortex-induced vibration and galloping.* Applied Physics Letters, 2018. **112**(3):

p. 033901.

59. Liu, F.-R., et al., *Y-type three-blade bluff body for wind energy harvesting.* Applied Physics Letters, 2018. **112**(23): p. 233903.
60. Wang, J., et al., *High-performance piezoelectric wind energy harvester with Y-shaped attachments.* Energy conversion and management, 2019. **181**: p. 645-652.
61. Levin, D. and E. Dowell. *Improving piezoelectric energy harvesting from an aeroelastic system*. in *International Forum on Aeroelasticity and Structural Dynamics IFASD*. 2019.
62. Gibbs, S., et al., *Flow field around the flapping flag.* Journal of Fluids and Structures, 2014. **48**: p. 507-513.
63. Shan, X., et al., *Enhancing the performance of an underwater piezoelectric energy harvester based on flow-induced vibration.* Energy, 2019. **172**: p. 134-140.
64. Zhang, B., et al., *Numerical investigation on VIV energy harvesting of bluff bodies with different cross sections in tandem arrangement.* Energy, 2017. **133**: p. 723-736.
65. Ding, L., et al., *Flow induced motion and energy harvesting of bluff bodies with different cross sections.* Energy Conversion and Management, 2015. **91**: p. 416-426.
66. Kwon, S.-D., *A T-shaped piezoelectric cantilever for fluid energy harvesting.* Applied physics letters, 2010. **97**(16): p. 164102.
67. Wang, J., et al., *Efficiency investigation on energy harvesting from airflows in HVAC system based on galloping of isosceles triangle sectioned bluff bodies.* Energy, 2019. **172**: p. 1066-1078.
68. Hu, G., et al., *Experimental investigation on the efficiency of circular cylinder-based wind energy harvester with different rod-shaped attachments.* Applied energy, 2018. **226**: p. 682-689.
69. Zhang, J., et al., *Flow induced vibration and energy extraction of an equilateral triangle prism at different system damping ratios.* Energies, 2016. **9**(11): p. 938.
70. Zhang, X., et al., *An arc-shaped piezoelectric bistable vibration energy harvester: Modeling and experiments.* Sensors, 2018. **18**(12): p. 4472.
71. Zhang, L., et al., *Improving the performance of aeroelastic energy harvesters by an interference cylinder.* Applied Physics Letters, 2017. **111**(7): p. 073904.
72. Kim, S., W.-X. Huang, and H.J. Sung, *Constructive and destructive interaction modes between two tandem flexible flags in viscous flow.* Journal of fluid mechanics, 2010. **661**: p. 511-521.
73. Huang, H., H. Wei, and X.-Y. Lu, *Coupling performance of tandem flexible inverted*

flags in a uniform flow. Journal of Fluid Mechanics, 2018. **837**: p. 461-476.

74. Huertas-Cerdeira, C., B. Fan, and M. Gharib, *Coupled motion of two side-by-side inverted flags.* Journal of Fluids and Structures, 2018. **76**: p. 527-535.
75. Zhao, L. and Y. Yang, *An impact-based broadband aeroelastic energy harvester for concurrent wind and base vibration energy harvesting.* Applied Energy, 2018. **212**: p. 233-243.
76. Choi, C.-K. and D.-K. Kwon, *Wind tunnel blockage effects on aerodynamic behavior of bluff body*. Wind Struct Int J, 1998. **1**(4): p. 351-364.
77. Latif, U.U., Emad & Younis, Yamin & Ali, Zaib & Sajid, Muhammad. , *Experimental electro-hydrodynamic investigation of flag-based energy harvesting in the wake of inverted C-shape cylinder.* . 2020.
78. Techet, A.H., J.J. Allen, and A.J. Smits. *Piezoelectric eels for energy harvesting in the ocean*. in *The twelfth international offshore and polar engineering conference*. 2002. OnePetro.
79. Michelin, S. and O. Doaré, *Energy harvesting efficiency of piezoelectric flags in axial flows.* Journal of Fluid Mechanics, 2013. **714**: p. 489-504.
80. Shoele, K. and R. Mittal, *Energy harvesting by flow-induced flutter in a simple model of an inverted piezoelectric flag.* Journal of Fluid Mechanics, 2016. **790**: p. 582-606.